

Comprehensive aerosol and gas data set from the Sydney Particle Study

Melita Keywood¹, Paul Selleck¹, Fabienne Reisen¹, David Cohen², Scott Chambers², Min Cheng¹, Martin Cope¹, Suzanne Crumeyrolle³, Erin Dunne¹, Kathryn Emmerson¹, Rosemary Fedele⁴, Ian Galbally¹, Rob Gillett¹, Alan Griffiths², Elise-Andree Guerette^{1,5}, James Harnwell¹, Ruhi Humphries¹, Sarah Lawson¹, Branka Miljevic⁶ Suzie Molloy¹, Jennifer Powell¹, Jack Simmons⁵, Zoran Ristovski⁶, Jason Ward¹

¹CSIRO Oceans and Atmosphere, Aspendale, VIC 3195, Australia

²ANSTO, Environmental Research, Kirrawee DC, NSW 2232, Australia

³Univ. Lille, Laboratoire d'Optique Atmosphérique, 59000 Lille, France

⁴EPA Victoria Melbourne Vic 3001 Australia

⁵University of Wollongong, School of Chemistry, NSW 2522, Australia

⁶Queensland University of Technology, School of Chemistry, Physics and Mechanical Engineering, Brisbane QLD 4001 Australia

Correspondence to: Melita Keywood (melita.keywood@csiro.au)

15 Abstract.

The Sydney Particle Study involved the comprehensive measurement of meteorology, particles and gases at a location in western Sydney during February/March 2011 and April/May 2012. The aim of this study was to increase scientific understanding of particle formation and transformations in the Sydney airshed. In this paper we describe the methods used to collect and analyse particle and gaseous samples, as well as the methods employed for the continuous measurement of particle concentrations, particle microphysical properties and gaseous concentrations. This paper also provides a description of the data collected and is a meta data record for the data sets published in Keywood et al. (2016a) <http://doi.org/10.4225/08/57903B83D6A5D> and Keywood et al. (2016b) <http://doi.org/10.4225/08/5791B5528BD63>.

1. Introduction

Atmospheric particles adversely effect human health, impacting mortality and morbidity (Pope et al., 2002), and are a significant contributor to outdoor air pollution being recognised by the World Health Organisation as carcinogenic to humans (Lim et al., 2012). Atmospheric particles are derived from a wide range of natural and anthropogenic sources, and hence are made up of a range of sizes and chemical compositions. This makes reduction of particle concentrations in the atmosphere by source regulation very challenging. In particular, reduction of secondary particles, which can be an important component of total particle exposure (Brook et al., 2010), are generated by photochemical reactions in the atmosphere and hence require control mechanisms that consider the relevant gas-phase precursors to these particles.

In the most recent Australian State of the Environment report, air quality standards were most often exceeded for fine particles in the capital cities, whilst ozone and nitrogen dioxide standards were not exceeded (Keywood et al., 2017). Currently, the highest episodes of particle pollution in Sydney can be ascribed to the presence of bushfire and dust plumes in the Sydney airshed (e.g. Johnston et al., 2011). However, significant increases in the frequency of hot days, drought and high fire risk weather have been projected for New South Wales, Australia (Whetton et al., 2015). The increased frequency of hot and sunny days has been linked to photochemical smog severity (Schnell and Prather 2017). Thus projected warmer conditions are likely to have implications for air pollution and health in New South Wales, Australia.

Comprehensive chemical transport modelling tools can be used to assist in the development of a long term control strategy for particles in the Sydney airshed. Such models should encompass comprehensive three-dimensional simulations of the atmosphere, sources and multi-phase chemistry that occurs, and should be informed by understanding of the contribution made by both local and remote particle sources to total particle exposure within the region. Ultimately such understanding should be underpinned by detailed and high quality experimental studies.

The Sydney Particle Study (SPS) aimed to increase scientific knowledge of the processes leading to particle formation and transformations in Sydney through two comprehensive observation programs. The groups that contributed to these observation programs included CSIRO, NSW Office of Environment and Heritage, ANSTO, Queensland University of Technology, the Shanghai Institute of Applied Physics and University of Wollongong. Observation made included the collection of samples for chemical analysis (aerosol composition, acid/alkaline gases, speciated volatile organic compounds [VOCs] including alkanes, aromatics, carbonyls, isoprene and monoterpenes). In addition, continuous or semi-continuous measurements were made of aerosol number size distributions, aerosol mass, aerosol light scattering, aerosol composition, and the gaseous criteria pollutants, oxides of nitrogen, carbon monoxide, sulfur dioxide and ozone [NO_x , CO, SO_2 , O_3]. Measurements were also made of meteorological parameters (wind speed, wind direction, temperature, relative humidity, radiation, boundary layer height) and atmospheric Radon-222 (radon) concentration.

2 Measurement Site

Measurements were made at the Westmead air quality station operated by the New South Wales Office of Environment and Heritage, located 24 km to the west of Sydney, Australia. The population of Sydney was 4.61 million in 2011 (ABS 2011), making Sydney the largest urban centre in Australia. Sydney is a coastal city with coastline to its east and elevated forested terrain (up to 1000 m) to the north, west and south. The climate is temperate with uniform rainfall, warm summers and cool winters.

The SPS observations occurred in two time periods; Summer 2011 (5 February - 7 March 2011 SPS-I) and autumn 2012 (16 April-14 May 2012 SPS-II).

3 Instruments and methods

The sampling program included the measurement of aerosols, criteria gases including NO_x, CO, SO₂ and ozone, acid/alkaline gases including NH₃, SO₂, HCl and HNO₃, speciated VOCs (including carbonyls), and meteorological parameters, including temperature, relative humidity (RH) and wind speed/direction and boundary layer height. Aerosols were measured with continuous or semi-continuous methods, including the measurement of aerosol mass, light scattering and number size distributions as well as integrated measurements of aerosol composition. Atmospheric radon concentration were also measured and provided as an indicator of transport and vertical mixing processes as described in Chambers et al. (2019).

Two integrated samples (particles, VOCs and acid/alkaline gas) were collected each day (morning 05:00 to 10:00 and afternoon 11:00 -19:00). Note that these times were local time (GMT+11 for SPS-I, GMT+10 for SPS-II). In addition, a third VOC sample was collected between 19:00 and 05:00 (i.e. overnight).

Table 1 provides a summary of the parameter measured and the instrument used to measure the parameter. The frequency at which the measurement of each parameter was made is also listed in the table ranging from continuous to one measurement every few minutes to the collection of a sample over several hours (integrated). The frequency at which the data are reported is also included in Table 1 as well as the units that the measurements are reported in, and estimate of the uncertainty of the measurement and whether the measurements were made during SPS-I, SPS-II or during both periods.

Table 1. Measurements made at Westmead during SPS-I and SPS-II along with the instrument or analytical technique employed, the measurement and reporting resolution, and the measurement units. Frequency of measurement is the frequency with which the data are collected. Frequency reported is the frequency at which the data are reported (may be an average of the frequency of measurement).

| Parameter | Instrument/ Analysis technique | Frequency of measurement | Frequency reported | Units | Estimate of Uncertainty | Study period |
|--|--|-----------------------------|-----------------------|--|----------------------------|-----------------|
| Number Size distribution 3-150 nm | Scanning mobility particle sizer (SMPS- Nano) with TSI 3085 DMA column and TSI 3776 Condensation Particle Counter (CPC) | 5 min | 5 min | dN/dLog dp particles cm ⁻³ | 20% | SPS-I |
| Number Size distribution 15 – 750 nm | SMPS-Long with TSI 3071A DMA and TSI 3010 CPC | 5 min | 5 min | dN/dLog dp particles cm ⁻³ | 20% | SPS-I |

| Parameter | Instrument/ Analysis technique | Frequency of measurement | Frequency reported | Units | Estimate of Uncertainty | Study period |
|---|--|--|-----------------------------|--|----------------------------|-------------------|
| Number Size distribution 15 – 750 nm | SMPS-Long with TSI 3081 DMA, TSI 3010 CPC and TSI controller (3080) | 2.5 min | 2.5 min | dN/dLog dp particles cm ⁻³ | 20% | SPS-II |
| Total particle number concentration | CPC TSI 3772 | continuous | 1 min | particles cm ⁻³ | 10% | SPS-I & SPS-II |
| Aerosol scattering coefficient | Integrating nephelometer Ecotech Aurora 1000G | continuous | 1 min | Mm ⁻¹ | 8% | SPS-I & SPS-II |
| PM _{2.5} , OC/EC, sugars (incl. Levoglucosan), water soluble ions | PM _{2.5} Ecotech 3000 high volume sampler / DRI Model 2001A Thermal-Optical Carbon Analyzer/Ion Chromatography | Integrated (2 samples per day) on all days | 05:00-10:00, 11:00-19:00 | µg m ⁻³ | 10-15% | SPS-I & SPS-II |
| PM _{2.5} elemental analysis | PM _{2.5} ASP Sampler/ Ion beam analysis ANSTO STAR 2MV accelerator | Integrated (2 samples per day) on all days | 05:00-10:00, 11:00-19:00 | µg m ⁻³ | 10% | SPS-II |
| PM ₁₀ | Thermo TEOM 1405 | Continuous | hourly | µg m ⁻³ | 7% | SPS-I & SPS-II |
| Radon | 700 L dual flow- loop two-filter radon detector | Continuous | 30 min and hourly | Bq m ⁻³ | 4% | SPS-I & SPS-II |
| CO | Ecotech EC9830 | Continuous | hourly | ppb | 10% | SPS-II |
| NO, NO ₂ , NO _x | Ecotech EC9841 | Continuous | hourly | ppb | 10% | SPS-I & SPS-II |

| Parameter | Instrument/ Analysis technique | Frequency of measurement | Frequency reported | Units | Estimate of Uncertainty | Study period |
|--|---|--|---|-----------------------|----------------------------|-------------------|
| Ozone | Ecotech EC9810 | Continuous | hourly | ppb | 10% | SPS-I & SPS-II |
| SO ₂ | Ecotech EC9850 | Continuous | hourly | ppb | 10% | SPS-I & SPS-II |
| NH ₃ , SO ₂ , HNO ₃ | Gas filter sampler/ Ion Chromatography | Integrated (2 samples/day) on all days | 05:00-10:00, 11:00-19:00 | ppb | 12% | SPS-I & SPS-II |
| VOCs | Proton transfer reaction mass spectrometry (PTR- MS) | Continuous | hourly | ppb | 10-22% | SPS-I & SPS-II |
| VOCs | adsorbent tube/GCMS | Integrated (3 samples/day) on all days | 05:00-10:00, 11:00-19:00, 19:00-05:00 | ppb | 7-13% | SPS-I & SPS-II |
| Carbonyls | S10 DNPH sampling/HPLC | Integrated (3 samples/day) on all days | 05:00-10:00, 11:00-19:00, 19:00-05:00 | ppb | 9-12% | SPS-I & SPS-II |
| Wind speed & wind direction | Met-One MET505 G4056 | Continuous | hourly | m s ⁻¹ & ° | 5% | SPS-I & SPS-II |
| Temperature & humidity | Vaisala HMP 155 | Continuous | hourly | °C & % | 3% (T), 7% (RH) | SPS-I & SPS-II |
| Solar | Middleton 8536 | Continuous | hourly | W m ⁻² | 5% | SPS-I & SPS-II |
| Boundary layer height | Leosphere ALS 450 lidar | 30 s | 20 min | m | 20% | SPS-II |

3.1 Continuous and semi-continuous measurements

3.1.1. Aerosol microphysical measurements

85 Aerosol size distributions were measured by different instruments during SPS-I and SPS-II. During SPS-I two instruments were used: a Scanning Mobility Particle Sizer (SMPS) which was custom built and included a long Differential Mobility Analyser (DMA, TSI 3071A) column and CPC (TSI 3010) (Long-SMPS) and a nano-SMPS which was also custom built and consisted of a short DMA (TSI 3085) column and CPC (TSI 3776) (Nano-SPMS). Both the Long-SMPS and Nano-SMPS were run with aerosol flows of 0.30 ± 0.03 L min⁻¹ and sheath flows of 3.0 ± 0.3 L min⁻¹ resulting in distribution of particles between 15 - 736 nm being measured with the Long-SMPS and the distribution of particles between 4.6-156 nm being

90 measured with the Nano-SMPS. Size distribution scans occurred over 5 minute intervals and PolyStyrene Latex (PSL) spheres were used to determine the sizing accuracy of both SMPS systems ($\pm 2\%$). Data were collected using TSI Aerosol Instrument Manager Software and analysed and processed using SMPS Loading and Processing Functions Version 1.8.8 authored by Tim Onasch from Aerodyne Research, Inc.

95 Comparison of the total number concentrations of particles greater than 10 nm measured with the Nano-SMPS to the particle number concentration measured using the CPC TSI3772 determined the counting efficiency of the Nano-SMPS and a scaling factor was determined which was then used to scale the Nano-SMPS size distributions. The Nano-SMPS and Long-SMPS had an overlap between 15 - 156 nm. The relationship between the concentrations measured in the overlapping size ranges was used to scale the Long-SMPS concentrations to the Nano-SMPS concentrations. Merging of the Long-SMPS and Nano-SMPS data sets produced a distribution between 4.6 - 736 nm.

100 During SPS-II aerosol size distributions were measured using an SMPS which included a long DMA column(DMA, TSI 3081) column and CPC (TSI 3010) and the TSI controller (3080). The SMPS was run with aerosol flows of $0.30 \pm 0.03 \text{ L min}^{-1}$ and sheath flows of $3.0 \pm 0.3 \text{ L min}^{-1}$ resulting in the distribution of particles between 15 - 736 nm. Size distributions scans occurred over 2.5 minute intervals and PolyStyrene Latex (PSL) spheres were used to determine the sizing accuracy of both SMPS systems ($\pm 2\%$). The counting efficiency of the SMPS was determined by comparing the total number concentration of
105 particles greater than 14 nm with the particle number concentration measured using the CPC TSI3772 and a scaling factor determined. The SMPS concentrations were then scaled to the scaling factor.

The estimated uncertainty listed in Table 1 was determined from the propagation of relative uncertainty of the aerosol and sheath flow rates, diameter calibration, uncertainty in the inversion procedures (estimated to be 10%) and uncertainty in the CPC counts (determined from the precision of several CPCs during intercomparison experiments). Figure 1 shows the time
110 series of particle concentration as a function of diameter (particle size distribution) for SPS-I and SPS-II.

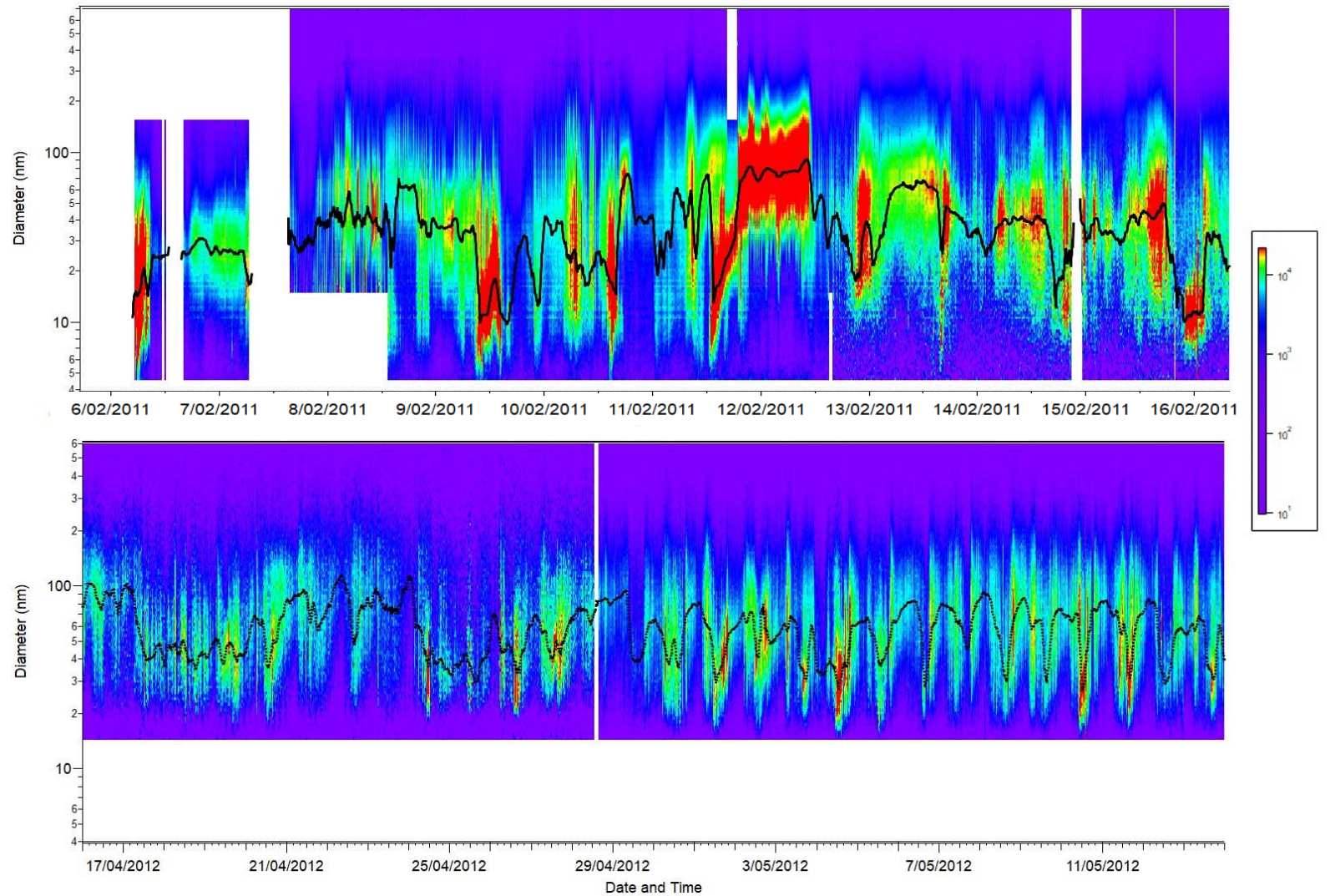


Figure 1 Time series of aerosol size distribution for SPS-I (top panel) and SPS-II (bottom panel). The black line on each plot is the mode diameter. Contour plots were produced using SMPS Loading and Processing Functions Version 1.8.8 authored by Tim Onasch from Aerodyne Research, Inc.

3.1.2 Aerosol scattering coefficient

During SPS-I and SPS-II aerosol scattering was measured at 525 nm using an integrating nephelometer (Ecotech Aurora 1000G). In this instrument, air is drawn into a chamber with a light beam at 525 nm and a photomultiplier detector set at right angles to the light beam. Particles in the air scatter the light beam. The detector measures the scattered light beam in the forward and backward direction. The nephelometer was operated according to the Australian Standard Method for integrated nephelometer (AS/NZS 3580.12.1:2015). The inlet to the nephelometer was heated to ensure the relative humidity of the sample stream was less than 40%. Daily zero air and span gas checks were carried out and the nephelometer was calibrated using CO₂ every three months. The estimated uncertainty listed in Table 1 was determined from the propagation of relative uncertainty in the calibration gas accuracy and uncertainties in humidity, temperature and pressure measurements specified in AS/NZS 3580.12.1:2015. Figure 2 shows the time series of aerosol scattering coefficient during SPS-I and SPS-II.

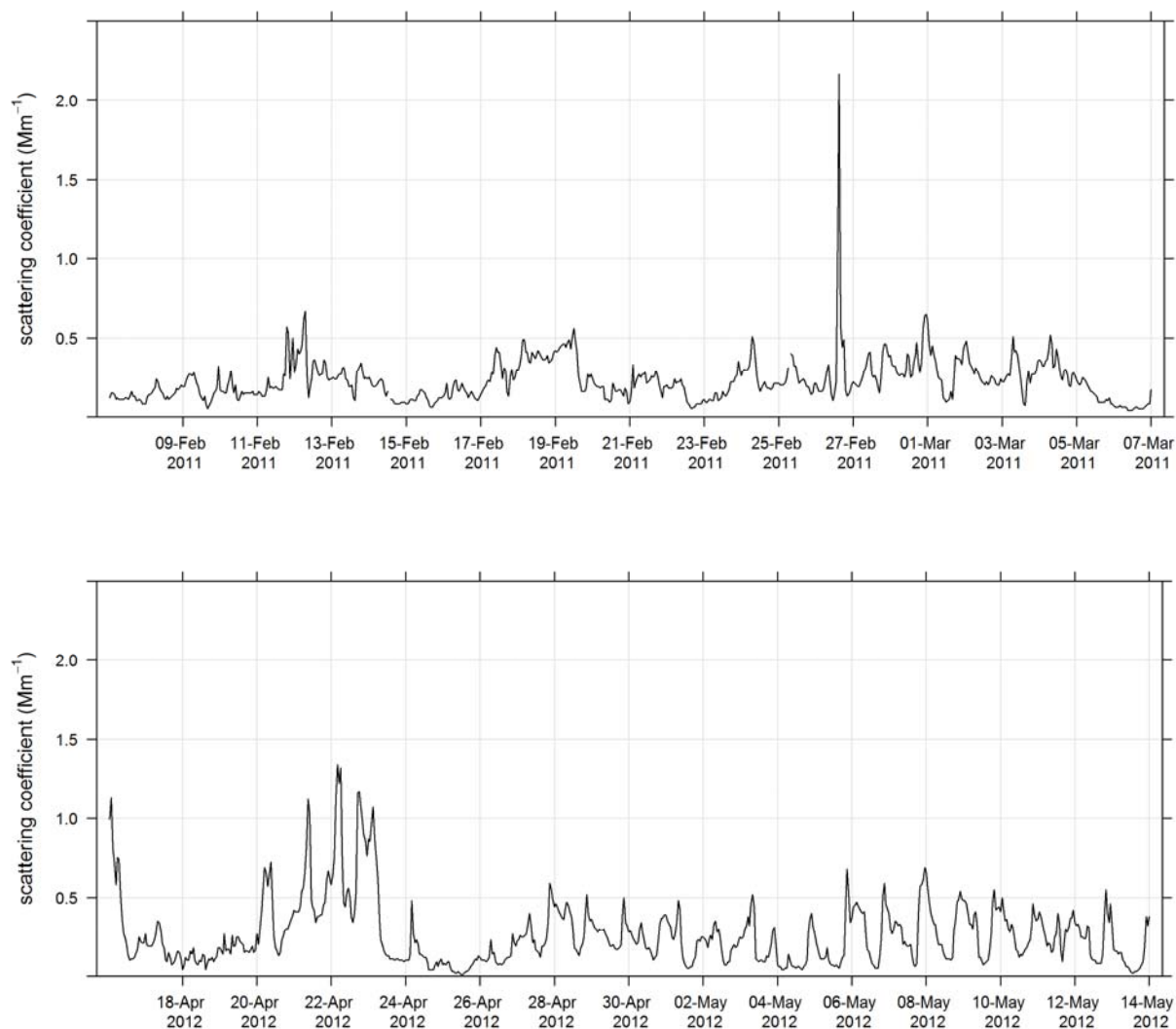
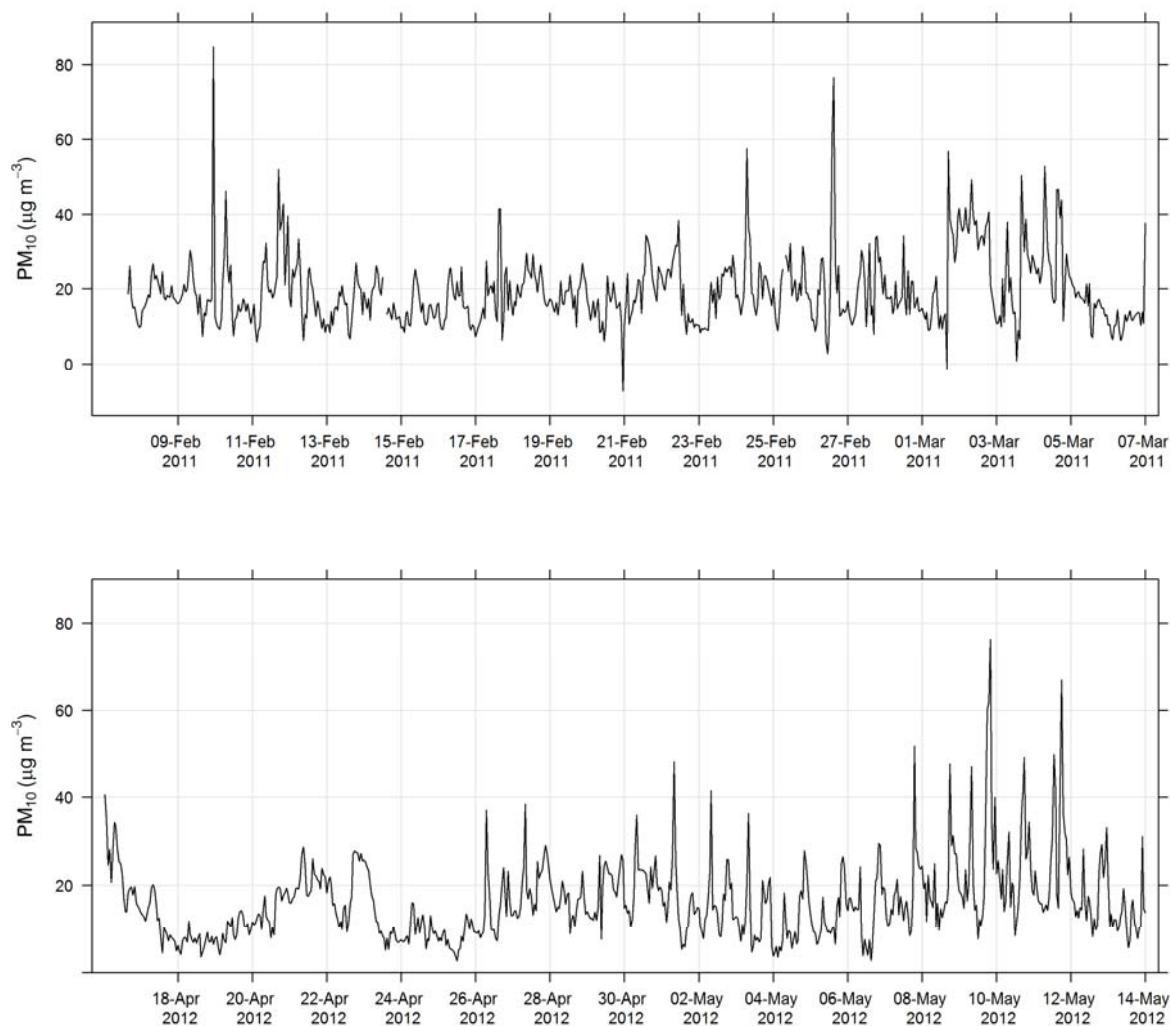


Figure 2 Time series of hourly averaged aerosol scattering coefficients during SPS-I (top panel) and SPS-II (bottom panel)

3.1.3 PM₁₀

130 During SPS-I and SPS-II the concentration of PM₁₀ was measured using a Tapered Element Oscillating Microbalance (Thermo TEOM1405). Air was drawn through a PM₁₀ impactor and a filter sitting on an oscillating microbalance. As mass loaded onto the filter, the frequency of oscillation changed and mass was recorded. The inlet to the TEOM was heated to 50 °C and the TEOM was operated according to Australian Standards for PM₁₀ continuous direct mass method using a tapered element oscillating microbalance analyser (AS/NZ 3580.9.8-2008). The estimated uncertainty listed in Table 1 was determined from

135 the propagation of relative uncertainties for flow rates, temperature, mass flow controllers and standard filter mass accuracy specified in AS/NZ 3580.9.8-2008. Figure 3 shows the time series of PM₁₀ during SPS-I and SPS-II.



140 **Figure 3** Time series of hourly averaged PM₁₀ concentrations during SPS-I (top panel) and SPS-II (bottom panel)

3.1.4 Proton transfer reaction mass spectrometer

Proton transfer reaction mass spectrometry (PTR-MS) is a chemical ionization mass spectrometry technique capable of quantifying volatile organic compounds (VOCs) in a gaseous sample at time resolutions down to a fraction of a second. The major constituents of air, oxygen, nitrogen, etc., are not detected. PTR-MS is suitable for the measurement of a range of atmospheric VOCs including aromatics, oxygenates, organo-sulphurs and terpenes.

145

The PTR-MS operates with the aid of a custom built auxiliary rack that regulates the flow of air in the sample inlet and controls whether the PTR-MS is sampling ambient or zero air or calibration gas. During this study zero readings and calibrations against certified gas standards were performed on the PTR-MS several times per day. Four calibration standards were used during the study, diluted to atmospheric concentrations using a set of mass flow controllers and a mixing chamber in the auxiliary rack.

150 The PTR-MS was calibrated for: formaldehyde, acetaldehyde, acrolein, methacrolein, acetone, methyl ethyl ketone, methanol, ethyl acetate, benzene, xylene, trimethyl benzene, isoprene, α -pinene, 1,8 cineole, dimethyl sulphide, acetonitrile and the mono-, di- and tri-chlorobenzenes. Only m/z that were detected above the method detection limit (MDL) greater than 25% of the time, and had peak to noise ratios greater than 5 (95th percentile/MDL) were reported. Further details are available in Galbally et al. (2007), Dunne et al. (2012) and Dunne et al. (2018). The estimated uncertainty listed in Table 1 was taken from Dunne et al. (2018).

155 et al. (2018). The time series of benzene, α -pinene and formaldehyde measured during SPS-I and SPS-II are shown in Figure 4 and Figure 5.

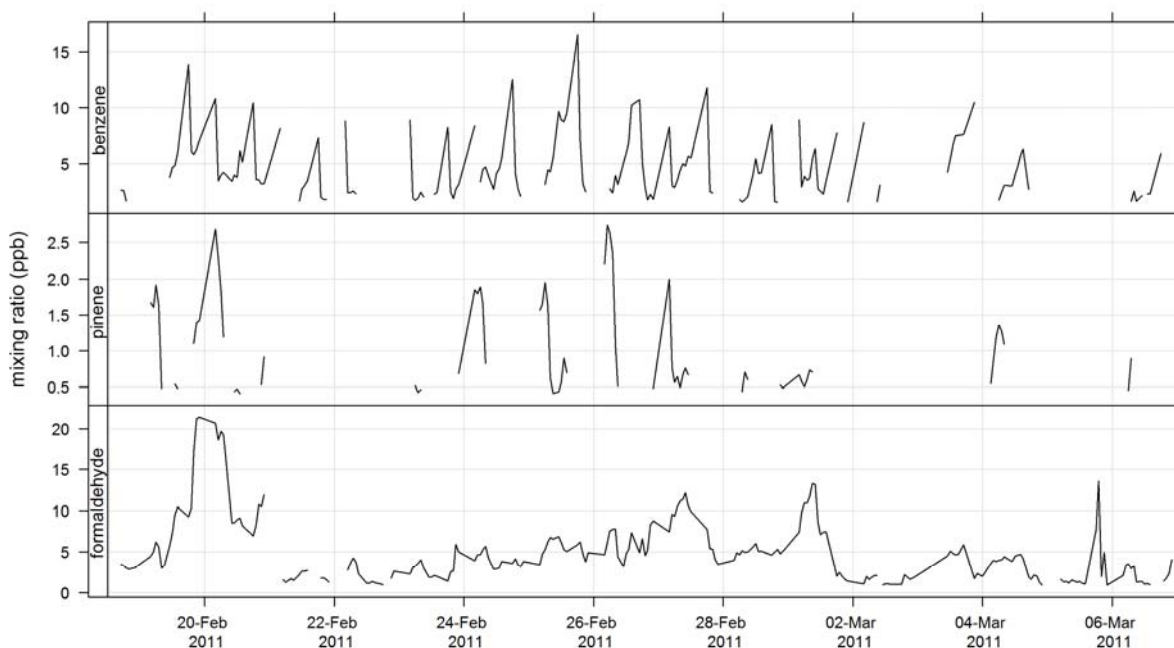
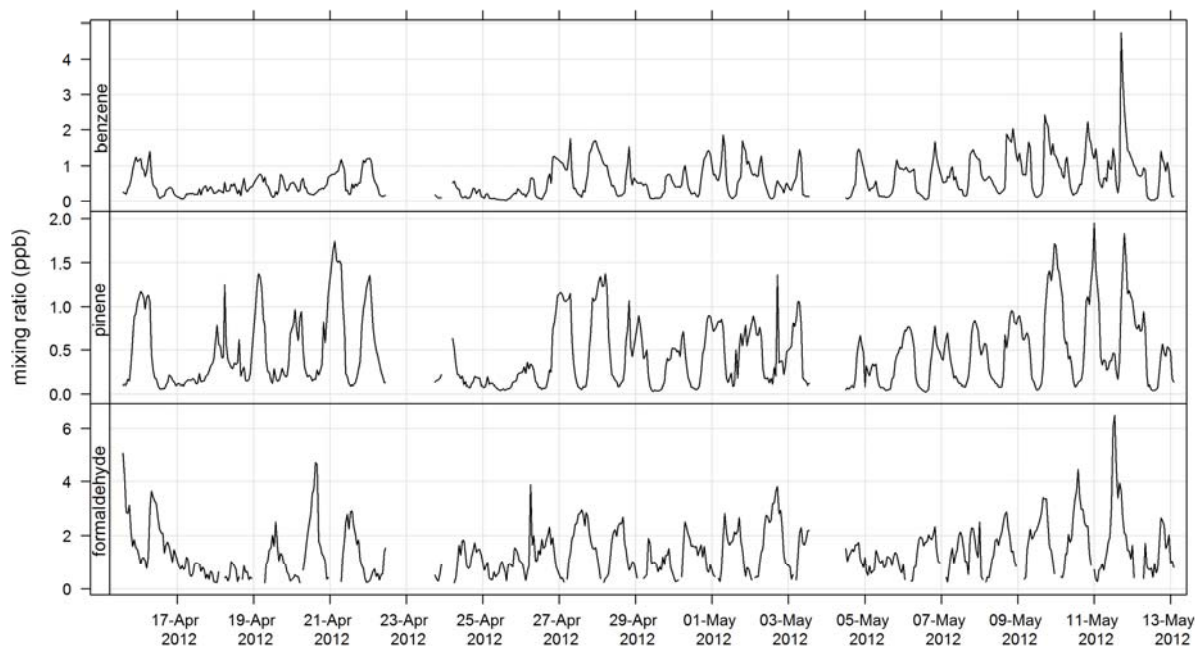


Figure 4 Time series of ambient benzene, α -pinene and formaldehyde mixing ratios during SPS-I measured with the PTR-MS



160 **Figure 5 Time series of ambient benzene, α -pinene and formaldehyde mixing ratios during SPS-II measured with the PTR-MS**

3.1.5 Radon

Radon concentration was measured using a dual flow-loop two-filter detection method (Whittlestone and Zahorowski, 1998; Chambers et al., 2014). The detector used for SPS-I and SPS-II was a 700 L model, which sampled at 40 L min^{-1} from 2 m above ground level (45 minute response time, $40\text{-}50 \text{ mBq m}^{-3}$ lower detection limit). Operation followed the approach
 165 described by Chambers et al. (2011). An on-site calibration was carried out using a NIST traceable Pylon Ra-226 source ($118.19 \pm 4\% \text{ kBq}$), and instrumental background checks were carried out pre and post deployment.

In addition to the raw detector output, a time series of the atmospheric radon concentration was computed by deconvolving the detector output, thereby correcting for the slow detector response (Griffiths et al., 2016). The deconvolved time series has larger statistical uncertainty than the uncorrected detector output, but is a better representation of the atmospheric radon
 170 concentration during periods when it is changing rapidly (e.g. during the morning transition between nocturnal and convective boundary layers). Figure 6 shows the time series of radon measured during SPS-I and SPS-II.

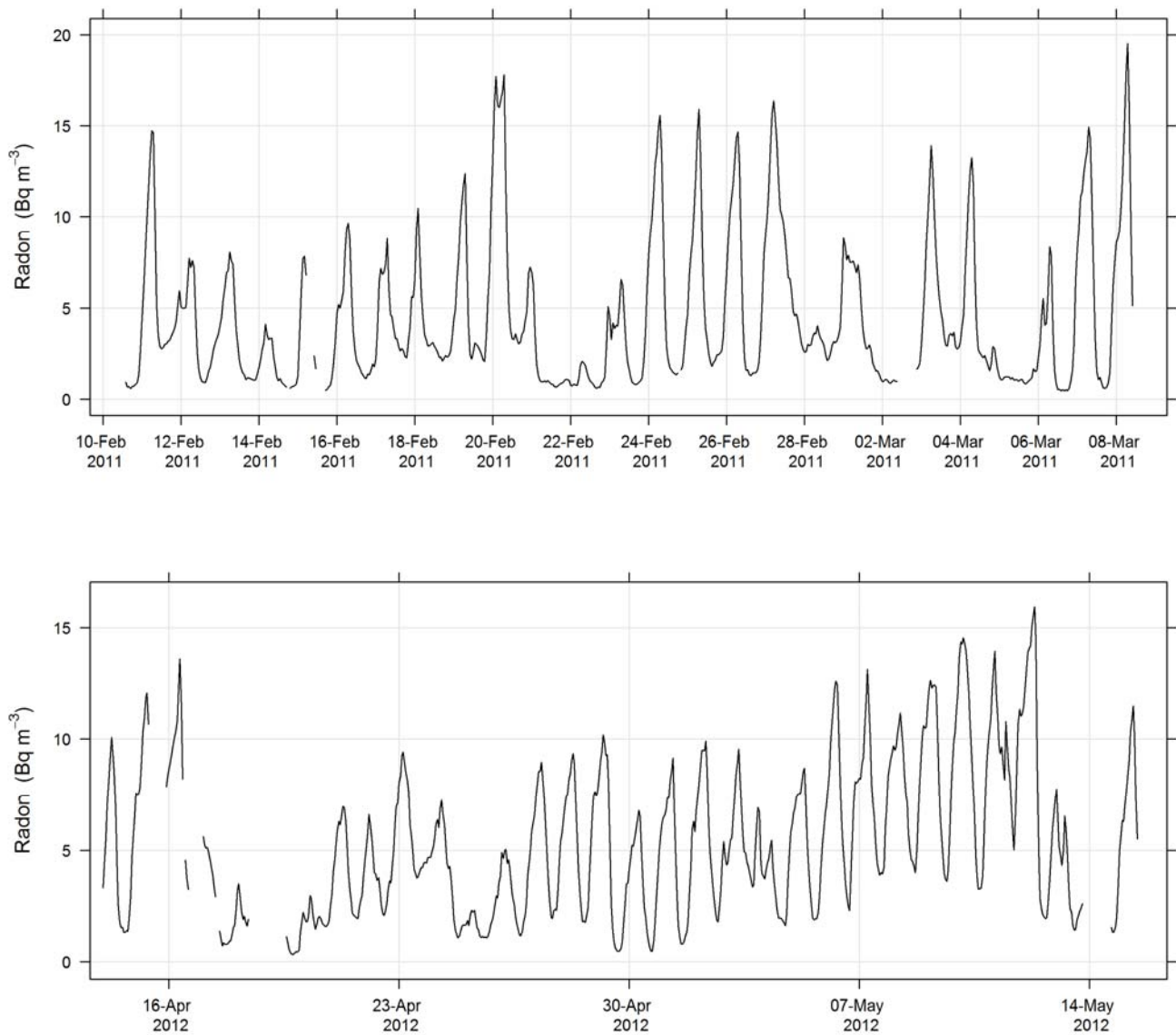


Figure 6 Time series radon concentrations during SPS-I and SPS-II.

175 **3.1.6 Criteria Gases**

Carbon Monoxide (CO) was measured using a nondispersive infrared CO analyser (Ecotech ML9830 CO trace gas analyser). In this instrument, sample air is drawn into a cell where a beam of infrared light is passed through it to a photodetector. The amount of light absorbed by CO in the sample is proportional to the number of molecules present, and the concentration of CO is determined by comparing the intensity of light measured by the photodetector with a cell containing a reference gas.

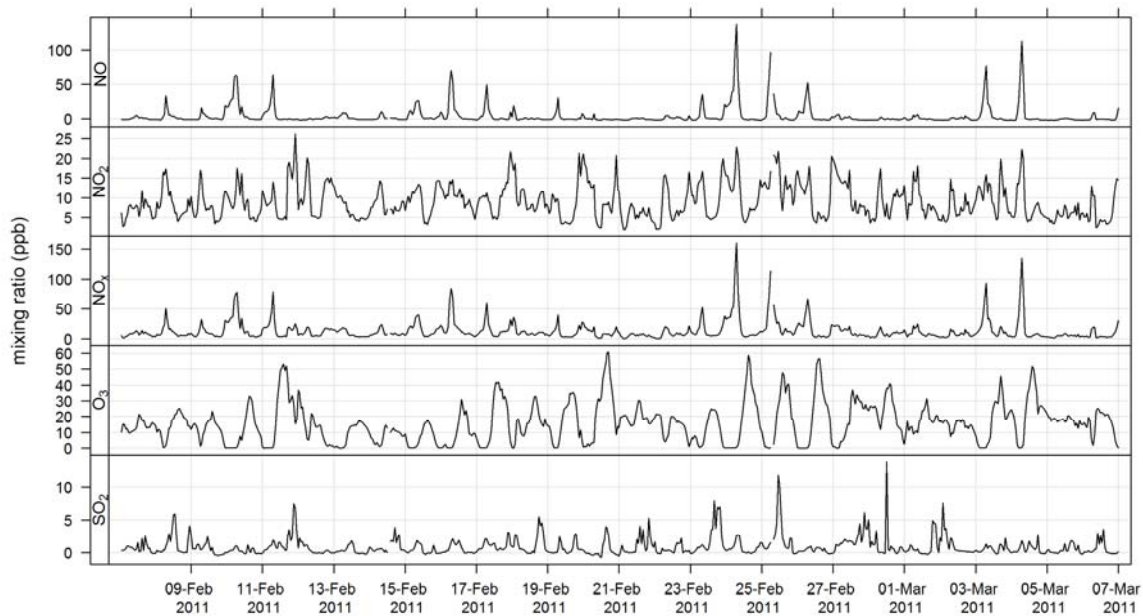
180 The CO analyser was operated according to the Australian Standard method for the determination of CO by direct-reading
instrumental method (AS/NZS 3580.7.1:2011). The estimated uncertainty listed in Table 1 is taken from AS/NZS
3580.7.1:2011.

Oxides of Nitrogen were measured using a chemiluminescent analyser (Ecotech EC9841 NO_x trace gas analyser). In this
instrument, nitric oxide (NO) in the sample air reacts with ozone (produced from an ultraviolet light) within a reaction chamber,
185 producing chemiluminescence in the wavelength range 600–3000 nm. The concentration of NO is proportional to the light
intensity measured by a photomultiplier tube. In a second sample stream, total nitrogen oxides (NO_x) are reduced to NO using
a selective converter. The concentration of nitrogen dioxide (NO₂) is assumed to be the difference between total NO_x and NO.
The analyser was operated according to the Australian standard method for the determination of oxides of nitrogen by direct-
reading instrumental method (AS/NZS 3580.5.1:2011). The estimated uncertainty listed in Table 1 is taken from AS/NZS
190 3580.5.1:2011.

Ozone (O₃) was measured using an ultraviolet spectrometer (Ecotech EC9810). In this instrument, a beam of ultraviolet light
is passed through the sample air within a cell containing an ultraviolet detector. The amount of light absorbed in the sample is
proportional to the number of O₃ molecules present and the decrease in light intensity determines the O₃ concentration in the
sample. The analyser was operated according to the Australian standard method for the determination of O₃ by direct-reading
195 instrumental method (AS/NZS 3580.6.1:2011). The estimated uncertainty listed in Table 1 is taken from AS/NZS
3580.6.1:2011.

Sulfur dioxide (SO₂) was measured by a pulsed fluorescence spectrophotometer (Ecotech EC9850). A stream of sample air is
drawn through a cell where it is exposed to pulsed ultraviolet light, resulting in excitation of SO₂ molecules. These molecules
subsequently fluoresce, by re-emitting light at a different wavelength. The intensity of the fluorescent light measured by a
200 photomultiplier tube, is proportional to the concentration of SO₂ in the sample air. The analyser was operated according to the
Australian standard method for the determination of SO₂ by direct-reading instrumental method (AS/NZS 3580.4.1:2008).
The estimated uncertainty listed in Table 1 is taken from AS/NZS 3580.4.1:2011.

The time series for CO, NO_x, O₃ and SO₂ for SPS-I and SPS-II are shown in Figure 7 and Figure 8.



205 **Figure 7** Time series of hourly averaged mixing ratios of criteria gases NO, NO₂, NO_x, O₃ and SO₂ during SPS-I

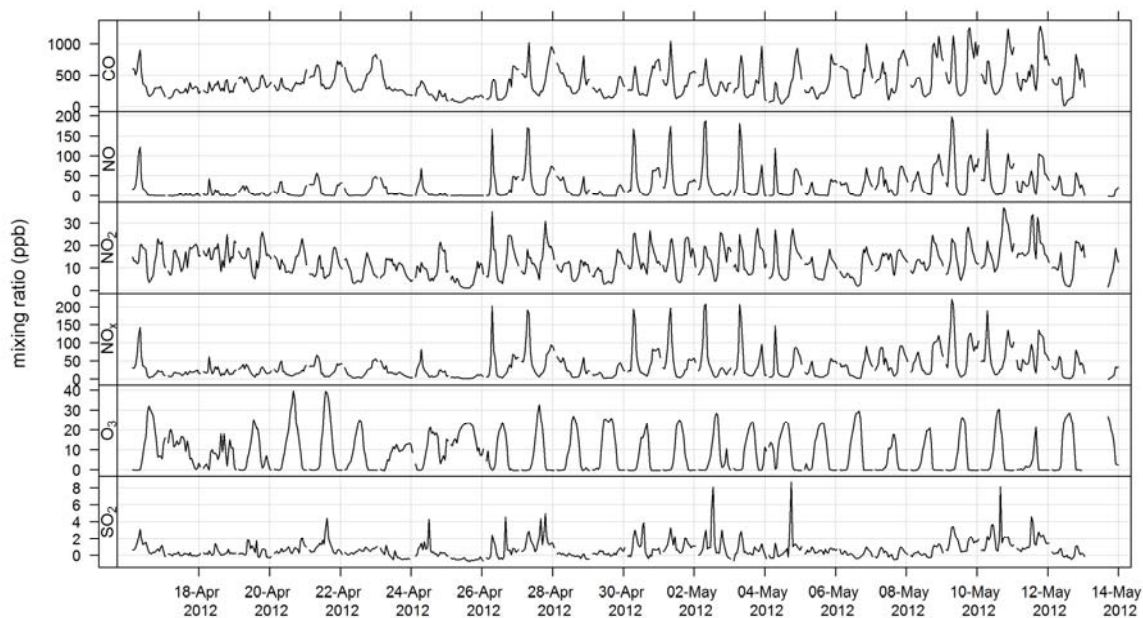


Figure 8 Time series of hourly averaged mixing ratios of criteria gases CO, NO, NO₂, NO_x, O₃ and SO₂ during SPS-II

3.1.7 Meteorology

- 210 An ultrasonic sensor (Met-One MET505) was used to measure wind speed and wind direction. Temperature and relative humidity were measured using a temperature and humidity probe (Vaisala HMP 155). Solar radiation was measured using a pyranometer (Middleton 8536). All instruments were sited and operated according to the Australian standard method for Meteorological monitoring for ambient air quality monitoring applications (AS/NZS 3580.14:2015). The estimated uncertainties listed in Table 1 are taken from AS/NZS 3580.14.1:2015.
- 215 The time series of temperature and relative humidity are shown for SPS-I in Figure 9, in addition solar radiation is also shown for SPS-II in Figure 10. The frequencies of wind speeds as a function of wind direction for SPS-I and SPS-II are shown in Figure 11.

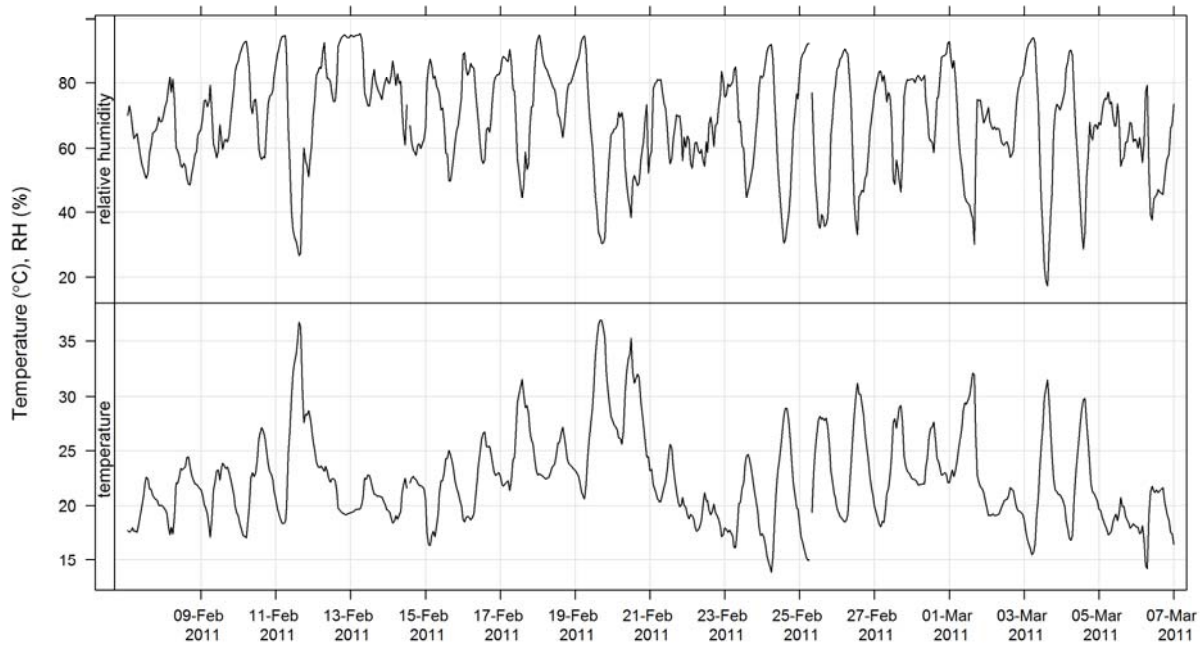
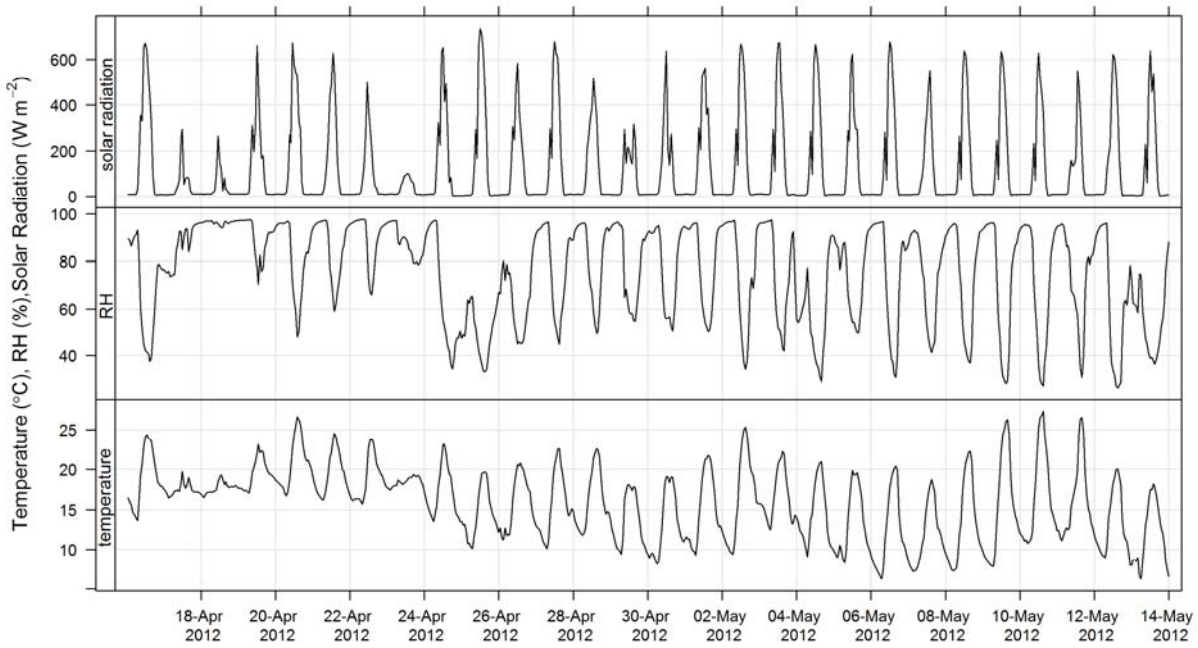


Figure 9 Time series of ambient temperature and relative humidity during SPS-I



220

Figure 10 Time series of ambient temperature, relative humidity and solar radiation during SPS-II

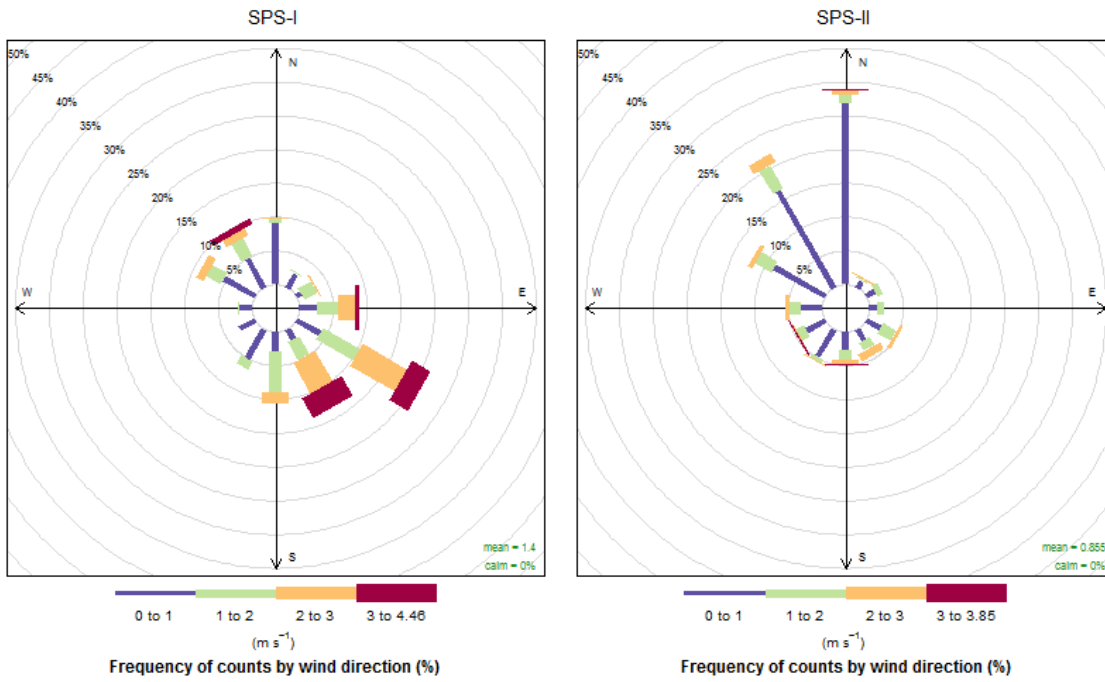


Figure 11 Wind roses during SPS-I in 2011 and SPS-II in 2012

225 **3.1.8 Lidar and boundary layer detection**

A Leosphere ALS 450 lidar was used to estimate cloud base, cloud top (for optically thin clouds) and the height of the boundary layer. The lidar incorporated a 355 nm UV laser that scattered light in the column of air back to a receiver. Raw data have a spatial resolution of 15 m and a temporal resolution of 30 s covering a range from about 200 m to 20 km. The physical basis for lidar remote sensing is described by Weitkamp (2005).

230 The conditions under which the lidar could determine the depth of the boundary layer included 1) the top of the boundary layer being deeper than about 200 m, and 2) accompanied by a sudden decrease in aerosol concentration. These conditions were most often met during daylight hours with clear skies or some fair weather cumulus.

Two approaches were combined in order to filter out periods with ambiguous retrievals of the boundary layer depth. The first method was an automated method, called STRAT-2D (Haeffelin et al., 2012), that used the Canny edge detection algorithm to detect discontinuities in the backscatter signal as a function of time and range. It is implemented in the STRAT analysis toolkit (Morille et al., 2007). The second method was a manual technique, in which the boundary layer top was detected by visual identification of the inflection point in a plot of $\log(Sr^2) \sim r$, where S is the received backscatter and r is the range from the lidar.

Based on the two estimates above, the boundary layer depth was computed by taking the average of the two estimates and assigning an uncertainty given by the range between the two estimates. Figure 12 shows the diurnal cycle in boundary layer depth measured during SPS-II.

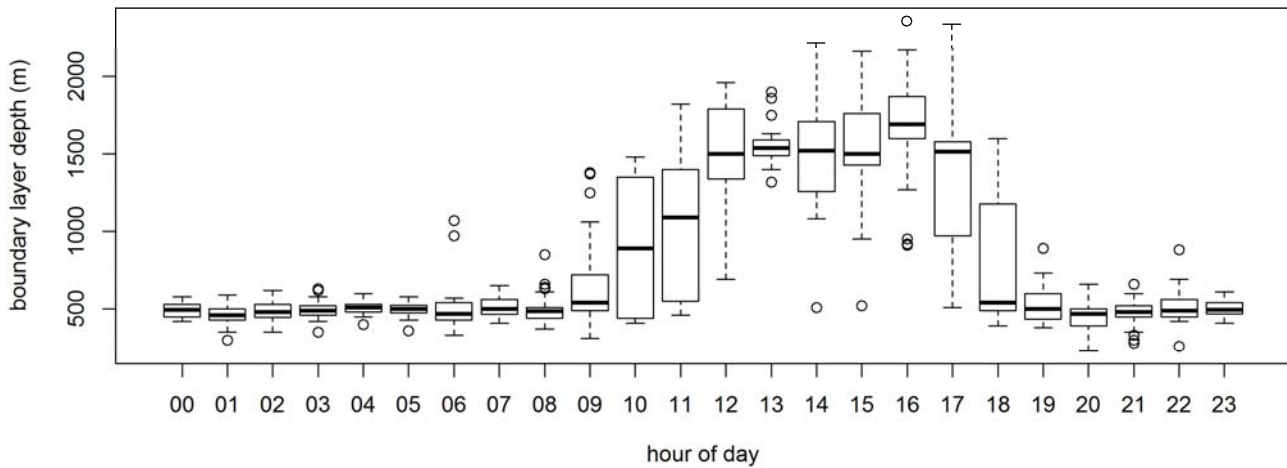


Figure 12 Boundary layer depth as a function of hour of the day for SPS-II

3.2 Integrated measurements

245 3.2.1 High Volume Sampler

In both SPS-I and SPS-II aerosol samples were collected using an Ecotech 3000 high volume sampler with a PM_{2.5} size-selective inlet (flow rate 67.8 m³ hr⁻¹ controlled with a mass flow controller, ambient temperature and pressure monitored so that both the ambient volumetric and standard flow rates were determined). Quartz membrane filters (250 mm x 200 mm Pall tissuequartz p/n 7204 prebaked at 600°C for 4 hours to reduce adsorbed organic vapours) were used to collect samples and
250 were stored in a freezer within sealed containers before and after sampling.

Throughout the study field blank samples (5 for SPS-I and 9 for SPS-II) were collected by running a pre-baked filter in the high volume sampler for 1 minute. Filter handling and analysis procedures were consistent for the field blanks and sample filters. In addition, to correct for sampling artefacts on the OC and EC concentrations, two filters were placed in the filter holder in sequence (front filter and back filter) for 20 of the SPS-I samples. The adsorption of volatile gases onto the filter
255 material results in positive artefacts, while degassing of semi-volatile compounds from the collected aerosol on the front filter which may be then absorbed onto the back filter, results in negative artefacts (Chow et al., 2010).

The filters were analysed for soluble ions using the method described in Section 3.3.1, and for OC and EC, the method described in Section 3.3.3.

3.2.2 Low Volume sampler

260 PM_{2.5} samples were collected using a sampler from the ANSTO Aerosol Sampling Program which includes a PM_{2.5} cyclone (flow rate 22 l min⁻¹). The cyclone is the same as that used in the US EPA IMPROVE network (<http://vista.cira.colostate.edu/improve/>). Thin 25 mm stretched Teflon filter were used to collect samples coincidentally with the high volume sampler to allow comparison of data during SPS-II. Samples were analysed for elemental concentrations using the method described in Section 3.3.2.

265 3.2.3 VOC and Carbonyls Sequencer

The VOC and Carbonyls Sequencer is an automatic continuous air sampler for sampling of VOC and carbonyls simultaneously. It has two channels: one for VOC and the other one for carbonyls. Each channel contains a sample inlet, 9 sampling ports, 4 solenoid valves and a sampling pump. A new sequencer was built for SPS-II that included a cooling system to keep the carbonyl tubes at 5-7 °C as well as extra sampling ports.

270 Samples were collected three times per day (05:00 – 10:00, 11:00 – 19:00 and 19:00 – 05:00) and during SPS-I a field blank (unopened tube) was collected each day. The new sequencer used in SPS-II incorporated additional sampling ports that were used to load extra sampling tubes that did not have any air sampled through them. These were then used as field blanks. The tubes were analysed for VOC concentrations using the method described in Section 3.3.5 and for carbonyls using the method described in Section 3.3.4.

275 3.2.4 Acid/Alkaline Gas sampler

The acid/alkaline gas sampler drew air through a 3-stage 47 mm filter pack at an ambient flow rate of 10 l min⁻¹. The first stage of the 3-stage filter pack contained a Teflon filter (Millipore fluoropore p/n FALP04700) to remove particles from the air stream, the second stage contained a sodium hydroxide coated quartz filter (Pall tissuequartz p/n 7202) to trap acidic gases and the final stage contained a citric acid coated quartz filter to trap alkaline gases. The filters were extracted in de-ionized water and analysed for soluble ion concentrations using the method described in Section 3.3.1.

3.3 Analysis methods

3.3.1 Ion chromatography

Suppressed ion chromatography (IC) and high-performance anion-exchange chromatography with pulsed amperometric detection (HPAEC-PAD) were used to measure water soluble ions and anhydrous sugars including levoglucosan (respectively) on a 6.25 cm² a portion of each quartz high volume sampler filter. De-ionized water (10 ml of 18.2 mΩ) was used to extract the quartz filter portions which were then preserved using 0.1 ml of chloroform. The acid and alkaline gas filter samples were also analysed by IC and the 47 mm filters were extracted in 3 ml of 18.2 mΩ de-ionized water and preserved with 0.03 ml of chloroform.

A Dionex ICS-3000 ion chromatograph was used to determine soluble ion (anion and cation) concentrations. The system included a Dionex AS17c analytical column (2 x 250 mm), an ASRS-300 suppressor and a gradient eluent of 0.75 mM to 35 mM potassium hydroxide to separate the anions, and a Dionex CS12a column (2 x 250 mm), a CSRS-300 suppressor and an isocratic eluent of 20 mM methanesulfonic acid to separate the cations. The species analysed were

- Chloride (Cl⁻)
- Nitrate (NO₃⁻)
- Sulphate (SO₄²⁻)
- Oxalate (C₂O₄⁻)
- Formate (HCOO⁻)
- Acetate (CH₃COO⁻)
- Phosphate (PO₄³⁻)
- Methanesulfonate (MSA⁻)
- Sodium (Na⁺)
- Ammonium (NH₄⁺)
- Magnesium (Mg²⁺)
- Calcium (Ca²⁺)
- Potassium (K⁺)

The estimated uncertainty listed in Table 1 was determined from the propagation of relative uncertainty associated with the collection of samples on the high volume sampler and the analytical method described here. The time series for Mg²⁺, Cl⁻ NH₄⁺ and SO₄²⁻ during SPS-I are shown in Figure 13 and those during SPS-II in Figure 14.

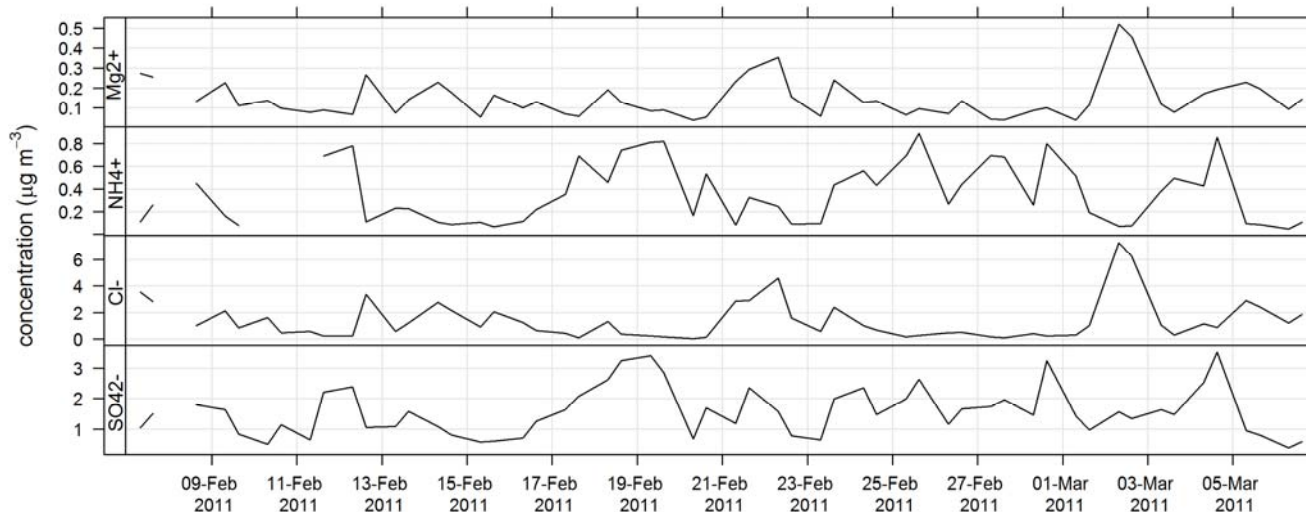


Figure 13 Time series of Mg^{2+} , Cl^- , NH_4^+ and SO_4^{2-} during SPS-I in 2011

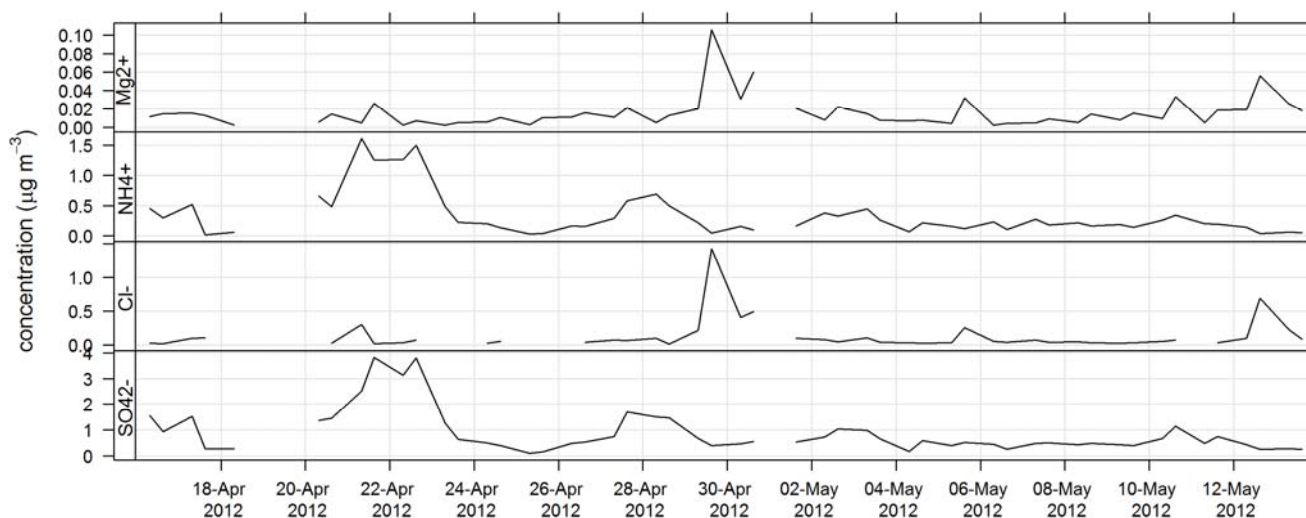


Figure 14 Time series of Mg^{2+} , Cl^- , NH_4^+ and SO_4^{2-} during SPS-II in 2012

300 An HPAEC-PAD with a Dionex ICS-3000 chromatograph with electrochemical detection was used to determine anhydrous sugar concentrations. The system was operated in the integrating (pulsed) amperometric mode using the carbohydrate (standard quad) waveform and utilizing disposable gold electrodes. A Dionex CarboPac MA 1 analytical column (4 x 250 mm) with a gradient eluent of 300 mM to 550 mM sodium hydroxide was used to separate the anhydrous sugars (Inuma et al.,

2009). The species analysed were levoglucosan ($C_6H_{10}O_5$, an anhydrous sugar - woodsmoke tracer) and Mannosan ($C_6H_{10}O_5$,
305 an anhydrous sugar - woodsmoke tracer). The time series of levoglucosan during SPS-I and SPS-II are shown in Figure 15.

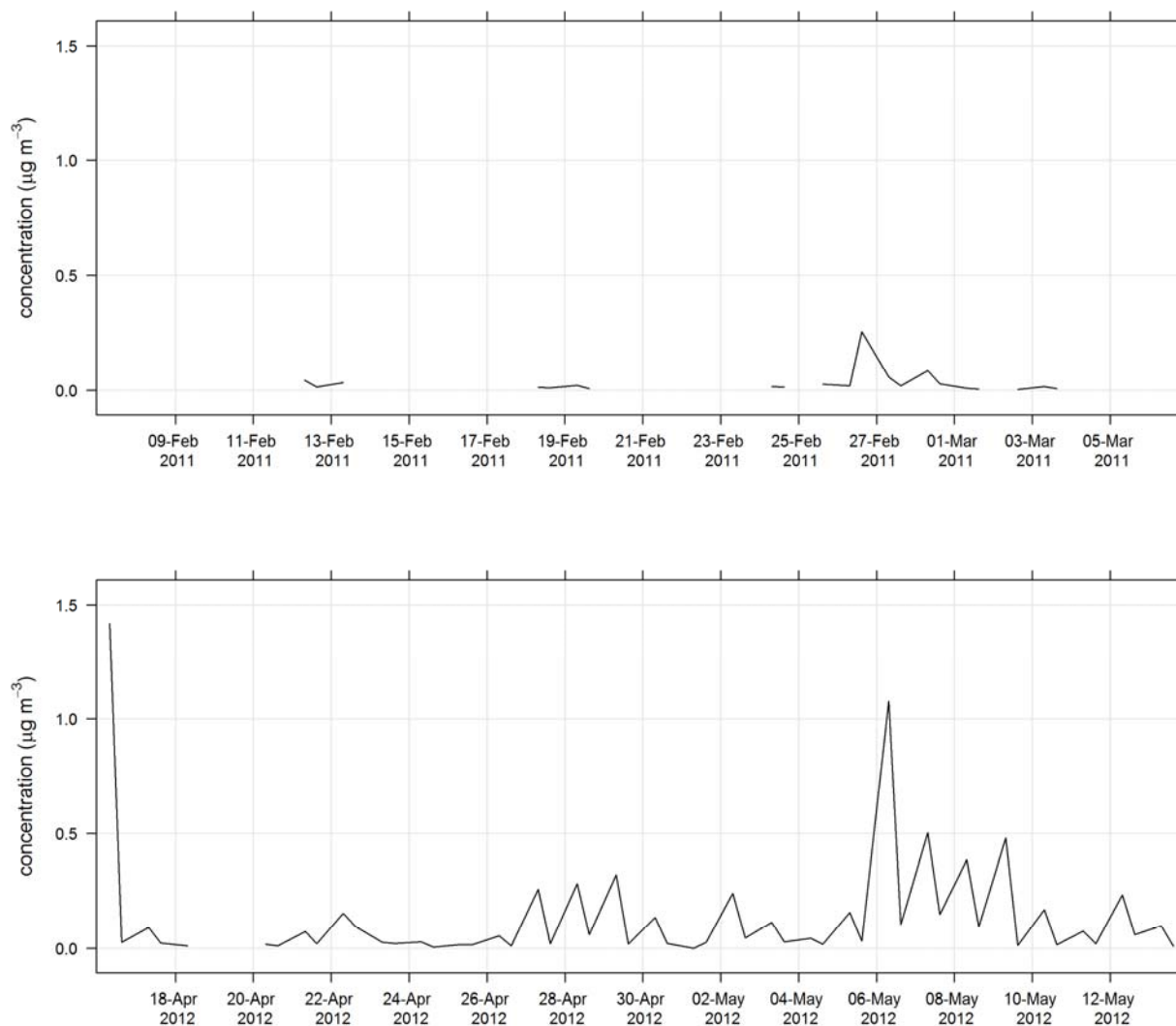


Figure 15 Time series of levoglucosan concentrations during SPS-I (top panel) and SPS-II (bottom panel)

3.3.2 Ion beam analysis

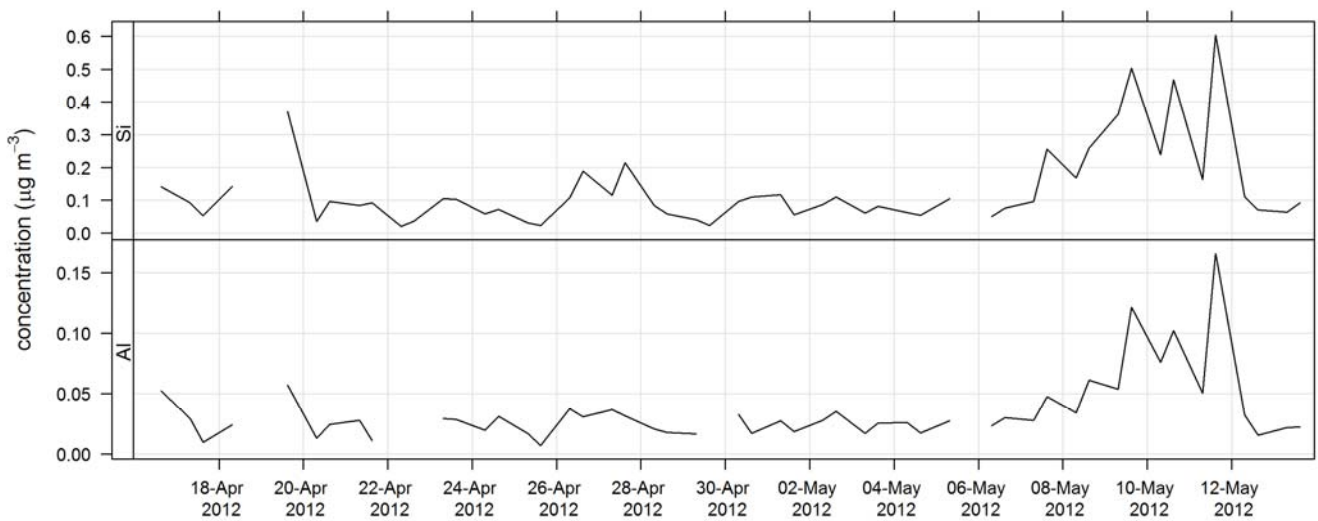
310 Nuclear ion beam analysis (IBA) techniques employing the non-destructive ANSTO STAR 2MV accelerator was used to determine the concentration of elements on the 25 mm Teflon filters collected by the low volume sampler. Analysis of aluminium to lead was carried out using Proton induced X-ray emission (PIXE see Cohen 1993 for details); analysis of light elements such as fluorine and sodium was carried out by Proton induced gamma-ray emission (PIGE see Cohen 1998 for

details) and analysis of hydrogen was carried out using Proton elastic scattering analysis (PESA see Cohen et al., 1996 for
315 details). Uncertainties reported in Cohen et al. (1996) include $\pm 14\%$ for sodium, $\pm 10\%$ for silicon and $\pm 7\%$ for hydrogen.

The elements determined were:

- Hydrogen (H)
- Sodium (Na)
- Aluminium (Al)
- Silicon (Si)
- Phosphorous (P)
- Sulfur (S)
- Chlorine (Cl)
- Potassium (K)
- Calcium (Ca)
- Titanium (Ti)
- Vanadium (V)
- Chromium (Cr)
- Manganese (Mn)
- Iron (Fe)
- Cobolt (Co)
- Nickel (Ni)
- Copper (Cu)
- Zinc (Zn)
- Bromine (Br)
- Lead (Pb)

The time series of Al and Si for SPS-II are shown in Figure 16.



320 **Figure 16 Time series of Al and Si during SPS-II**

3.3.3 Organic carbon and Elemental carbon analysis

A Desert Research Institute Model 2001A Thermal-Optical Carbon Analyzer was used to determine the concentration of
elemental carbon (EC) and organic carbon (OC) on a portion of the quartz filters collected using PM_{2.5} high volume sampler.
The IMPROVE-A temperature protocol (Chow et al., 2007) was employed and included using laser reflectance to correct for
325 charring. Before analysis the oven was baked to 910°C for 10 minutes to remove residual carbon and system blank levels were
then tested until $< 0.20 \mu\text{g C cm}^{-2}$ was reported (with repeat oven baking if necessary). Calibration checks were performed

twice daily to monitor possible catalyst degeneration. The analyser is reported to measure carbon concentrations between 0.05 – 750 $\mu\text{g C cm}^{-2}$, with uncertainties in OC and EC of $\pm 10\%$.

330 Four OC fractions at four non-oxidizing heat ramps (OC1 = 140°C, OC2 = 280°C, OC3 = 480°C, OC4 = 580°C) and three EC fractions at three oxidizing heat ramps (EC1 = 580°C, EC2 = 740°C, EC3 = 840°C) are measured in the IMPROVE-A carbon method. The sum of the different OC fractions and the OCpyro (the OC that was pyrolyzed which was measured from the reflectance of the filter) determined total OC. The sum of the EC fractions minus OCpyro determined total EC. The time series for OC and EC during SPS-I are shown in Figure 17 and the time series for OC and EC during SPS-II are shown in Figure 18.

335

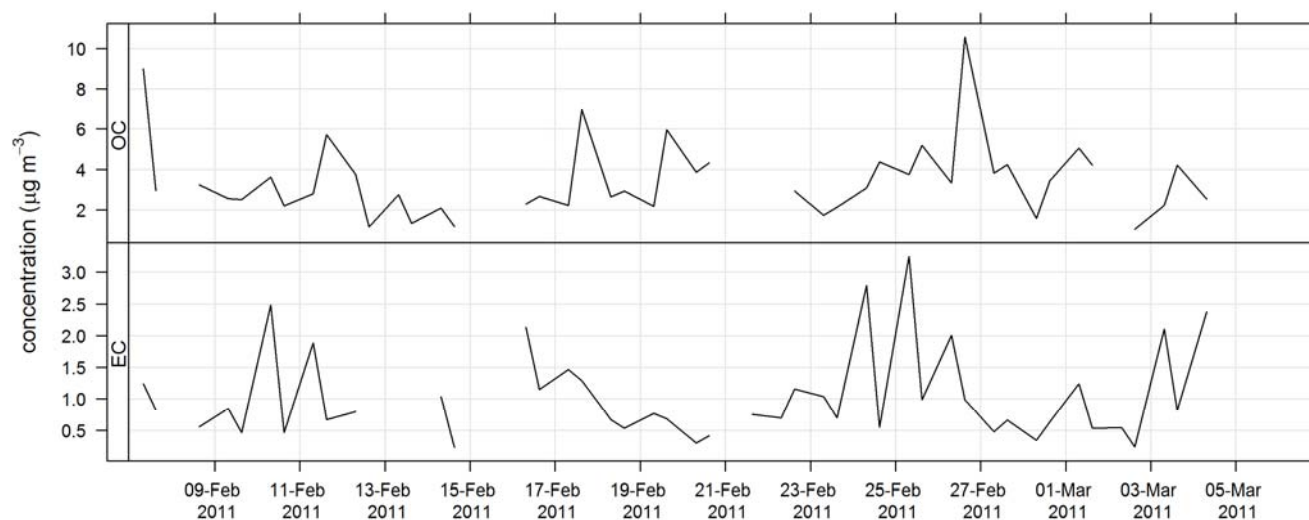


Figure 17 Time series of OC and EC during SPS-I in 2011

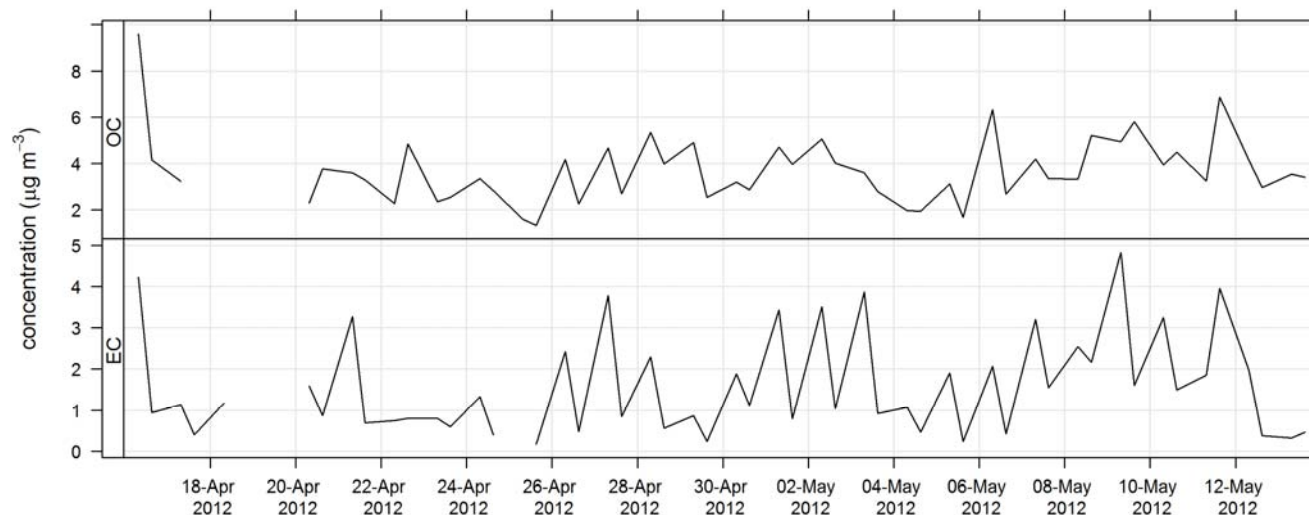


Figure 18 Time series of OC and EC during SPS-II in 2012

340 **3.3.4 Carbonyls analysis**

Carbonyls were collected by the sequencer onto cartridges (Supelco LpDNPH S10 p/n 21014) containing high-purity silica adsorbent coated with 2,4-dinitrophenylhydrazine (DNPH), where they were converted to the hydrazone derivatives. Samples were refrigerated immediately after sampling until analysis. The derivatives were extracted from the cartridge in 2.5 mL of acetonitrile and analysed by high performance liquid chromatography (HPLC) with diode array detection (DAD). The DAD enables the absorption spectra of each peak to be determined. The difference in the spectra highlights which peaks in the chromatograms are mono- or dicarbonyl DNPH derivatives and, along with retention times, allows the identification of the dicarbonyls glyoxal and methylglyoxal. Further details of this method can be found in Lawson et al. (2015). The estimated uncertainty listed in Table 1 was taken from Dunne et al. (2018). The time series of methylglyoxal and formaldehyde for SPS-I is shown in Figure 19 and time series of methylglyoxal and formaldehyde during SPS-II are shown in Figure 20.

350

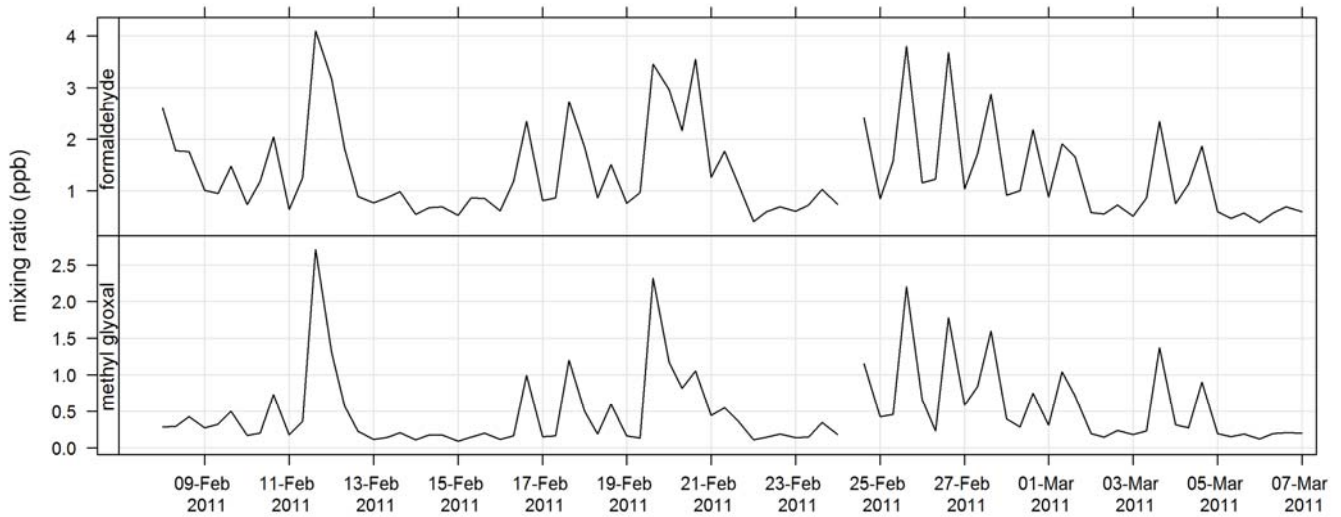


Figure 19 Time series of ambient formaldehyde and methylglyoxal mixing ratios during SPS-I

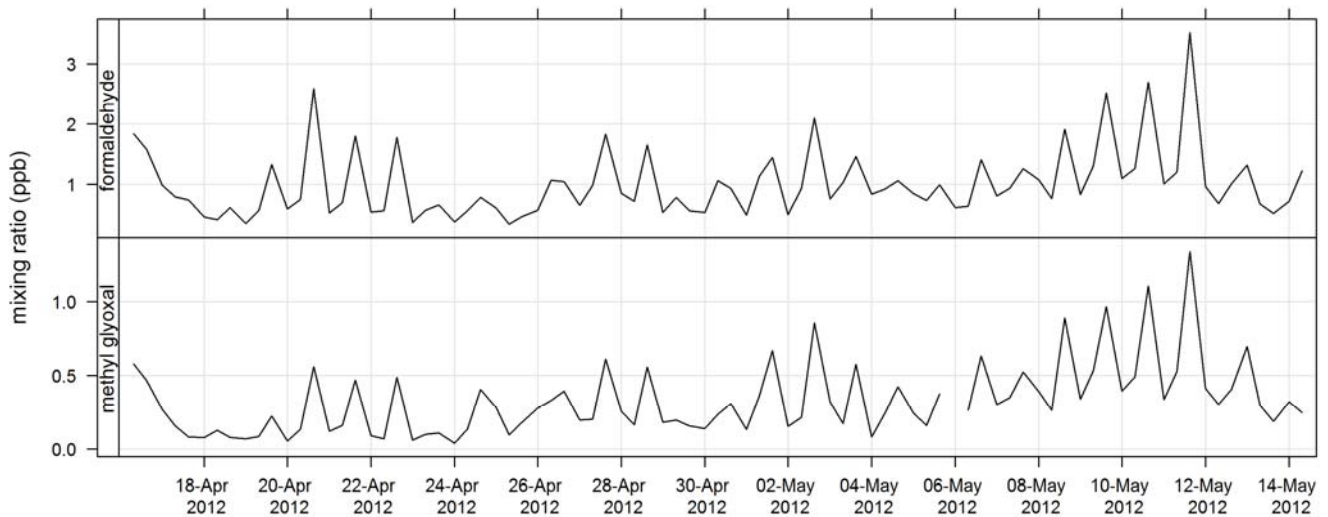
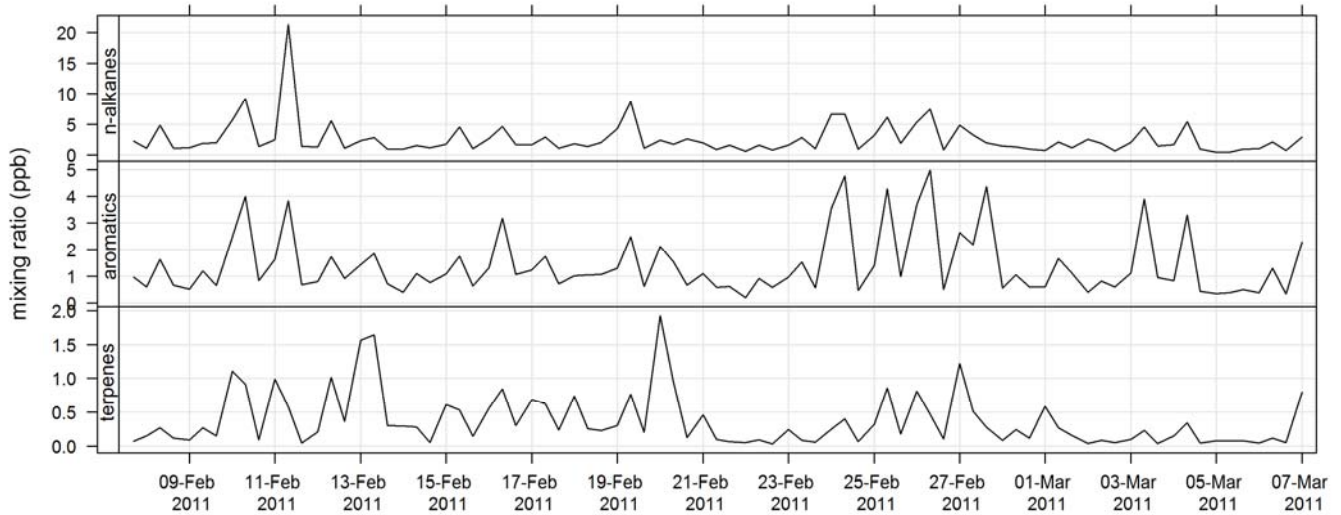


Figure 20 Time series of ambient formaldehyde and methylglyoxal mixing ratios concentrations during SPS-II

355 **3.3.5 Volatile organic compounds analysis**

An automatic Volatile organic compound (VOC) sampler was used collect VOC samples by actively drawing air through two adsorbent tubes in series (Markes Carbograph 1TD / Carbopack X) which were then analysed by a PerkinElmer TurboMatrix™ 650 ATD (Automated Thermal Desorber) and a Hewlett Packard 6890A gas chromatograph (GC) equipped with a Flame

Ionization Detector (FID) and a Mass Selective Detector (MSD). Calibration was via certified BTEX (benzene, toluene, ethylbenzene and xylenes), TO 15/17, terpenes, alcohols and PAM gas standards (Cheng et al., 2016). The method of AT (adsorbent tube) VOC sampling and analysis in this study was compatible with ISO16017-1:2000 (ISO 2000) and according to USEPA Compendium method TO-17 (USEPA TO-17). The estimated uncertainty listed in Table 1 was taken from Dunne et al. (2018). The time series for total alkane, aromatic and terpene concentrations for SPS-I are shown in Figure 21 and for SPS-II in Figure 22.



365

Figure 21 Time series of total alkane, total aromatics and total terpene mixing ratios during SPS-I in 2011 measured on absorbent tubes

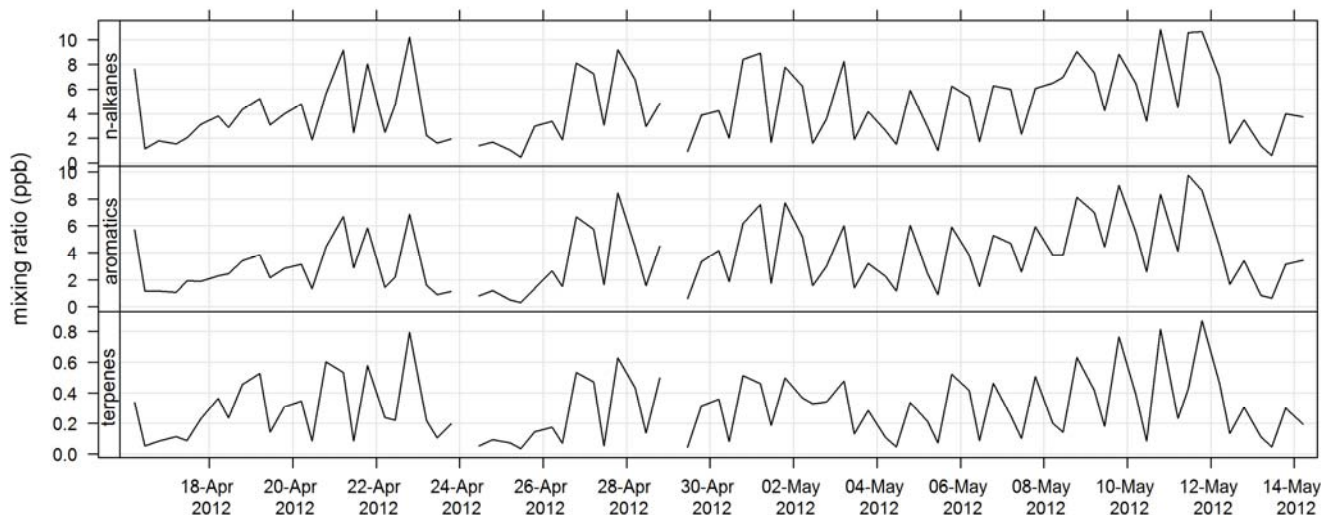


Figure 22 Time series of total alkane, total aromatic and total terpene mixing ratios during SPS-II in 2012 measured on absorbent tubes

370 4. Aerosol composition

The factors that determine the composition of aerosols are the source of the aerosols (or precursor gases) and subsequent transformations that occur in the atmosphere or within the aerosol themselves. As such the sources of aerosols may be inferred from the chemical composition of the aerosol samples. A detailed analysis of the aerosol composition data is beyond the scope of a paper in this journal. Instead, presented here are the data for some species that can be used as markers for different aerosol sources.

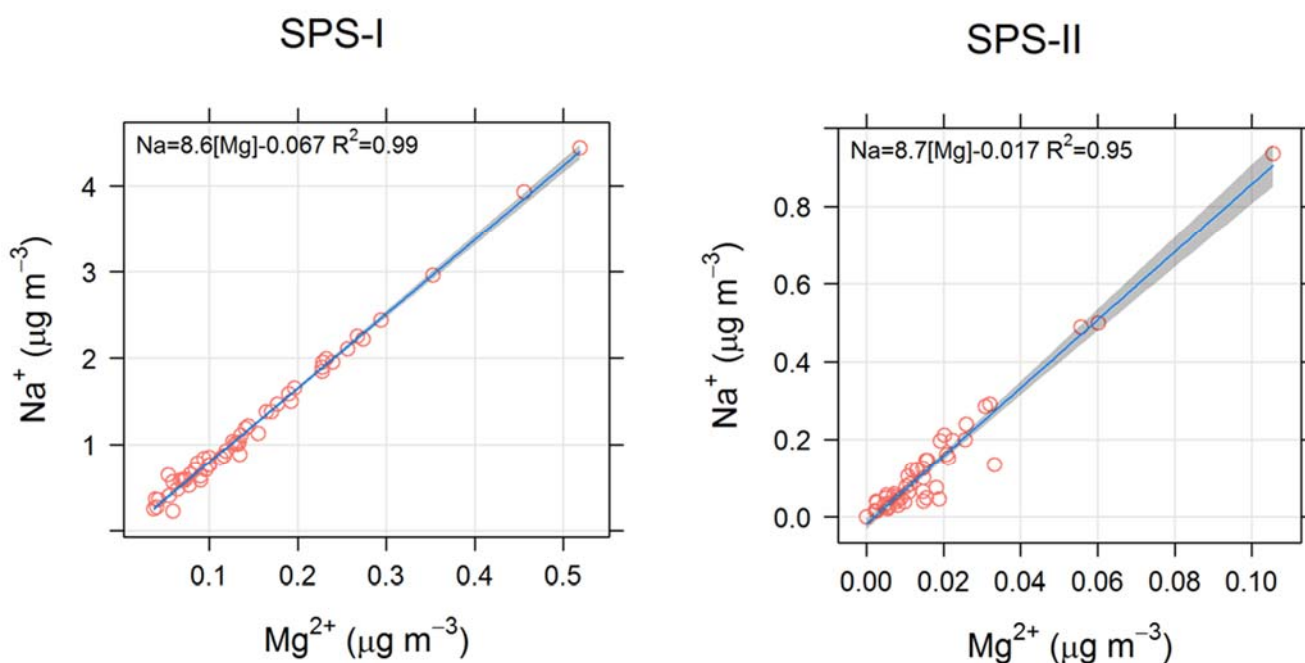
375 Table 2 lists the markers that can be used to trace different aerosol sources. In some instances, a chemical species is a unique tracer for a source. For example, levoglucosan is a unique tracer for biomass burning (Simoneit et al., 1999; Simoneit 2002). The time series of levoglucosan for both sampling periods is shown in Figure 15. Concentrations were generally greater in SPS-II than SPS-I, indicating a greater contribution of biomass burning, most likely woodheaters used for domestic heating

380 during autumn in Sydney in SPS-II. In addition the ratios of different species may provide information about an aerosol source. For example a sea-salt source may be indicated by a $[Na^+/Mg^{2+}]$ ratio close to 8.3 (Millero et al., 2008), and an Australian crustal dust source may be indicated by a $[Si/Al]$ ratio of close to 3.08 (Radhi et al., 2010). Figure 23 shows the relationship between Na^+ and Mg^{2+} for SPS-I and SPS-II, suggesting that the ratio of these species is close to that of sea-salt. Figure 24 shows the relationship between Si and

385 Al for SPS-II. The slope of 4 shown in the regression line is similar to that measured by Radhi et al. (2010), indicative of Australian dusts.

Table 2. Sources and their indicator species

| Source | Indicator Species |
|--|--|
| Soil | Non sea-salt Calcium (SPS-I) |
| | Silicon, Iron, Aluminium , Titanium (SPS-II) |
| Organic Matter (OM) – Vehicles, Industry, Biomass Burning (BB), secondary organic aerosol (SOA) | Organic Carbon |
| Elemental Carbon (EC)- Vehicles, Industry, BB | Elemental Carbon |
| Sea-Salt | Sodium, Chloride, Magnesium |
| Secondary Inorganic Aerosol (SIA) | Non sea-salt Sulfate , Ammonium Nitrate |
| Biomass Burning (BB) | Levoglucosan |



390

Figure 23 Scatter plot of Mg and Na for SPS-1 (left) and SPS-II (right)

SPS-II

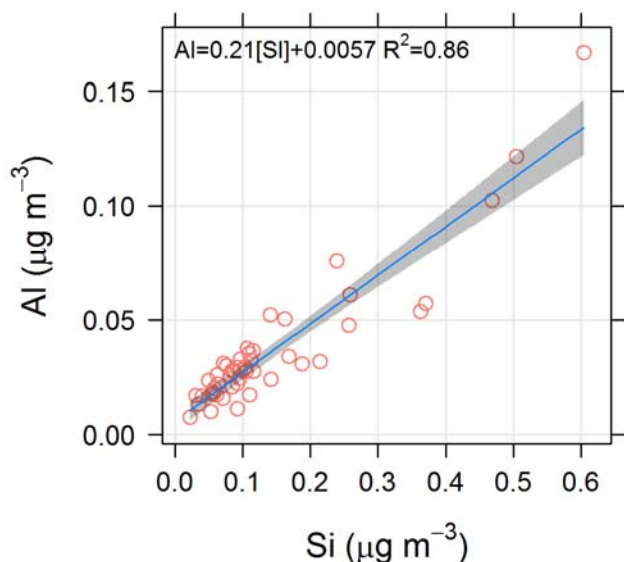


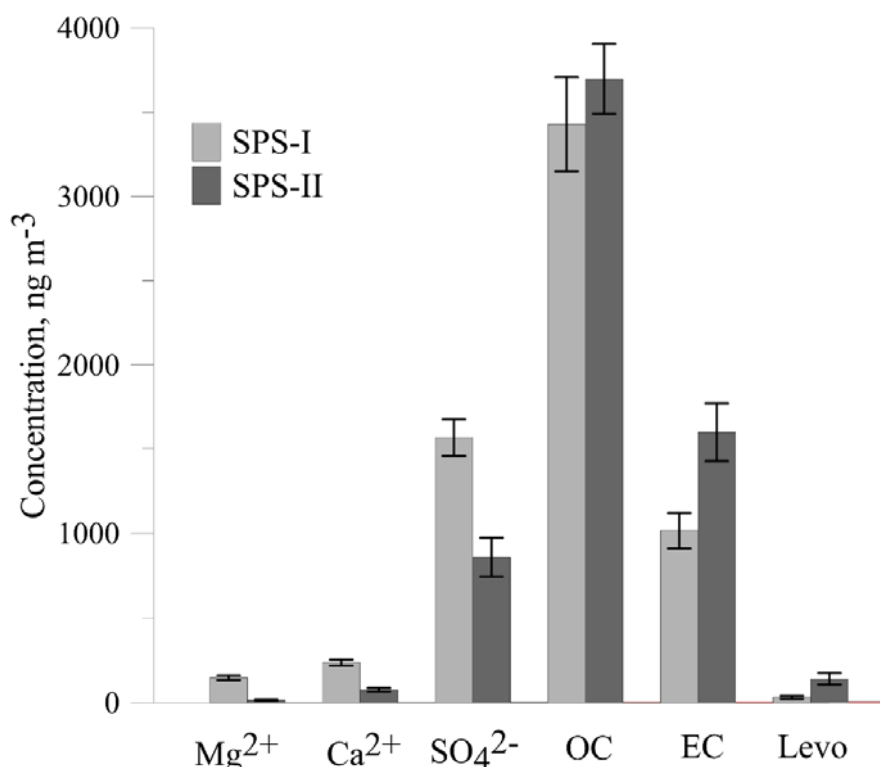
Figure 24 Scatter plot of Al and Si for SPS-II

395 Many compounds, however, may be derived from more than one source (e.g. EC can be present in vehicles emissions, industrial emissions and biomass burning) and when sufficient sample numbers allow (generally more than 100) receptor modelling methodologies can be used to apportion sources to the aerosol loadings (Norris et al., 2008). During both SPS-I and SPS-II 30 samples were collected in the mornings and 30 in the afternoons. Hence with only 60 samples for each sampling period, we are restricted to a qualitative and rudimentary assessment of aerosol sources utilising information on relationships
400 between some key marker species and the timing of their occurrence.

The time series for EC, OC, SO_4^{2-} , Mg^{2+} and Ca^{2+} are shown above. The average concentrations for SPS-I and SPS-II for each of these species are shown in Figure 25. A marker for sea-salt, Mg^{2+} and a marker for soil, non sea-salt Ca^{2+} , show higher concentrations during SPS-I (summer). Higher non sea-salt sulfate concentrations during SPS-I (summer), a marker for secondary aerosol during summer may indicate greater secondary aerosol production during summer. Levoglucosan (the
405 marker for woodsmoke) and EC show highest concentrations during the SPS-II (autumn). The average OC concentration is not significantly different between SPS-I and SPS-II.

Higher sea-salt and soil marker species in summer than autumn may be due to higher wind speeds observed during SPS-I since both sea-salt and dust are mechanically produced aerosol. Figure 11 also showed there to be a greater recent oceanic fetch in summer; and during summer soils in rural regions are drier, and covered with less vegetation, so therefore more mobile. Higher
410 secondary aerosol marker species in summer may indicate more photochemical aerosol production in summer, while higher

biomass burning marker species in autumn may represent a greater contributions from woodheaters to the aerosol loading during this time of the year. Converse to the higher wind speeds during summer, the lower windspeeds during autumn are conducive to the build-up of pollutants during autumn which will also influence the concentrations of EC and levoglucosan during autumn. As noted above, a quantitative assessment of aerosol sources influencing the airshed during SPS-I and SPS-II 415 could be carried out using a receptor modelling approach if more samples had been collected.



420 **Figure 25 Comparison of average concentrations of Mg (a marker for sea-salt), Ca (a marker for soil), SO₄ (a marker for secondary aerosol), OC, EC and levo = levoglucosan (biomass burning marker) during SPS-I and SPS-II. Error bars represent standard error (standard deviation/square root of number of observations). Mg, Ca, and SO₄ are significantly greater during SPS-I (p <<0.05), OC is not significantly different between SPS-I and SPS-II (p=0.4), EC and levoglucosan are significantly greater during SPS-II (p= 0.003 EC and p=0.004 levoglucosan).**

5 Data set repository and description

The data sets for both SPS-I and SPS-II are stored on the Commonwealth Scientific and Industrial Research Organisation 425 (CSIRO) data access portal. The SPS-I data set is available at Keywood et al. (2016a) <http://doi.org/10.4225/08/57903B83D6A5D> and the SPS-II data set is available at Keywood et al. (2016b) <http://doi.org/10.4225/08/5791B5528BD63>.

6 Acknowledgements

Descriptive and statistical analyses were carried out using R statistical analysis version 3.5.1 (R Core Team, 2016). The main
430 package used in R statistical analysis is known as “openair” version 2.4.2 (Carslaw and Ropkins, 2012). These projects was
partially funded by grants from the New South Wales Office of Environment.

7 References

- ABS: Product 3235.0 - Population by Age and Sex, Regions of Australia, 2011
435 [http://www.abs.gov.au/ausstats/abs@.nsf/Products/3235.0~2011~Main+Features~New+South+Wales?OpenDocum
ent](http://www.abs.gov.au/ausstats/abs@.nsf/Products/3235.0~2011~Main+Features~New+South+Wales?OpenDocument), 2011.
- AS/NZ 3580.9.8-2008: Determination of suspended particulate matter—PM10 continuous direct mass method using a tapered
element oscillating microbalance analyser, 2008.
- AS/NZS 3580.12.1:2015: Methods for sampling and analysis of ambient air - Determination of light scattering - Integrating
nephelometer method, 2015.
- 440 AS/NZS 3580.14:2014: Methods for sampling and analysis of ambient air - Part 14: Meteorological monitoring for ambient
air quality monitoring applications, 2014.
- AS/NZS 3580.4.1:2008: Methods of Sampling and Analysis of Ambient Air – Determination of sulfur dioxide- Direct reading
instrumental method., 2008.
- AS/NZS 3580:5.1:2011: Methods of Sampling and Analysis of Ambient Air – Determination of oxides of nitrogen- Direct
445 reading instrumental method., 2011.
- AS/NZS 3580:6.1:2011: Methods of Sampling and Analysis of Ambient Air – Determination of ozone- Direct reading
instrumental method., 2011.
- AS/NZS 3580:7.1:2011: Methods of Sampling and Analysis of Ambient Air – Determination of carbon monoxide- Direct
reading instrumental method., 2011.
- 450 Brook, R. D., Rajagopalan, S., Pope, C. A., Brook, J. R., Bhatnagar, A., Diez-Roux, A. V., Holguin, F., Hong, Y. L., Luepker,
R. V., Mittleman, M. A., Peters, A., Siscovick, D., Smith, S. C., Whitsel, L., Kaufman, J. D., Amer Heart Assoc
Council, E., Council Kidney Cardiovase, D., and Council Nutr Phys Activity, M.: Particulate Matter Air Pollution
and Cardiovascular Disease An Update to the Scientific Statement From the American Heart Association, *Circulation*,
121, 2331-2378, 10.1161/CIR.0b013e3181dbee1, 2010.
- 455 Carslaw DC, and Ropkins K: openair — An R package for air quality data analysis.” *Environmental Modelling & Software*,
27–28(0), 52–61. ISSN 1364-8152, doi: 10.1016/j.envsoft.2011.09.008. , 2012.
- Chambers, S., Williams, A. G., Zahorowski, W., Griffiths, A., and Crawford, J.: Separating remote fetch and local mixing
influences on vertical radon measurements in the lower atmosphere, *Tellus Series B-Chemical and Physical
Meteorology*, 63, 843-859, 10.1111/j.1600-0889.2011.00565.x, 2011.
- 460 Chambers, S. D., Hong, S. B., Williams, A. G., Crawford, J., Griffiths, A. D., and Park, S. J.: Characterising terrestrial
influences on Antarctic air masses using Radon-222 measurements at King George Island, *Atmospheric Chemistry
and Physics*, 14, 9903-9916, 10.5194/acp-14-9903-2014, 2014.
- Chambers, S. D., Guerette, E. A., Monk, K., Griffiths, A. D., Zhang, Y., Duc, H., Cope, M., Emmerson, K. M., Chang, L. T.,
Silver, J. D., Utembe, S., Crawford, J., Williams, A. G., and Keywood, M.: Skill-Testing Chemical Transport Models
465 across Contrasting Atmospheric Mixing States Using Radon-222, *Atmosphere*, 10, 25 10.3390/atmos10010025,
2019.
- Cheng, M., Galbally, I. E., Molloy, S. B., Selleck, P. W., Keywood, M. D., Lawson, S. J., Powell, J. C., Gillett, R. W., and
Dunne, E.: Factors controlling volatile organic compounds in dwellings in Melbourne, Australia, *Indoor Air*, 26, 219-
230, 10.1111/ina.12201, 2016.

- 470 Chow, J. C., Watson, J. G., Chen, L. W. A., Chang, M. C. O., Robinson, N. F., Trimble, D., and Kohl, S.: The IMPROVE-A temperature protocol for thermal/optical carbon analysis: maintaining consistency with a long-term database, *J. Air Waste Manage. Assoc.*, 57, 1014-1023, 10.3155/1047-3289.57.9.1014, 2007.
- Chow, J. C., Watson, J. G., Chen, L. W. A., Rice, J., and Frank, N. H.: Quantification of PM_{2.5} organic carbon sampling artifacts in US networks, *Atmospheric Chemistry and Physics*, 10, 5223-5239, 10.5194/acp-10-5223-2010, 2010.
- 475 Cohen, D. D.: APPLICATIONS OF SIMULTANEOUS IBA TECHNIQUES TO AEROSOL ANALYSIS, *Nuclear Instruments & Methods in Physics Research Section B-Beam Interactions with Materials and Atoms*, 79, 385-388, 10.1016/0168-583x(93)95368-f, 1993.
- Cohen, D. D., Bailey, G. M., and Kondepudi, R.: Elemental analysis by PIXE and other IBA techniques and their application to source fingerprinting of atmospheric fine particle pollution, *Nuclear Instruments & Methods in Physics Research Section B-Beam Interactions with Materials and Atoms*, 109, 218-226, 10.1016/0168-583x(95)00912-4, 1996.
- 480 Cohen, D. D.: Characterisation of atmospheric fine particles using IBA techniques, *Nuclear Instruments & Methods in Physics Research Section B-Beam Interactions with Materials and Atoms*, 136, 14-22, 10.1016/s0168-583x(97)00658-7, 1998.
- Dunne, E., Galbally, I. E., Lawson, S., and Patti, A.: Interference in the PTR-MS measurement of acetonitrile at m/z 42 in polluted urban air-A study using switchable reagent ion PTR-MS, *International Journal of Mass Spectrometry*, 319, 40-47, 10.1016/j.ijms.2012.05.004, 2012.
- 485 Dunne, E., Galbally, I. E., Cheng, M., Selleck, P., Molloy, S. B., and Lawson, S. J.: Comparison of VOC measurements made by PTR-MS, adsorbent tubes-GC-FID-MS and DNPH derivatization-HPLC during the Sydney Particle Study, 2012: a contribution to the assessment of uncertainty in routine atmospheric VOC measurements, *Atmospheric Measurement Techniques*, 11, 141-159, 10.5194/amt-11-141-2018, 2018.
- 490 Galbally, I. E., Lawson, S. J., Weeks, I. A., Bentley, S. T., Gillett, R. W., Meyer, M., and Goldstein, A. H.: Volatile organic compounds in marine air at Cape Grim, Australia, *Environmental Chemistry*, 4, 178-182, 10.1071/en07024, 2007.
- Griffiths, A. D., Chambers, S. D., Williams, A. G., and Werczynski, S.: Increasing the accuracy and temporal resolution of two-filter radon-222 measurements by correcting for the instrument response, *Atmospheric Measurement Techniques*, 9, 2689-2707, 10.5194/amt-9-2689-2016, 2016.
- 495 Haeffelin, M., Angelini, F., Morille, Y., Martucci, G., Frey, S., Gobbi, G. P., Lolli, S., O'Dowd, C. D., Sauvage, L., Xueref-Remy, I., Wastine, B., and Feist, D. G.: Evaluation of Mixing-Height Retrievals from Automatic Profiling Lidars and Ceilometers in View of Future Integrated Networks in Europe, *Boundary-Layer Meteorology*, 143, 49-75, 10.1007/s10546-011-9643-z, 2012.
- 500 Iinuma, Y., Engling, G., Puxbaum, H., and Herrmann, H.: A highly resolved anion-exchange chromatographic method for determination of saccharidic tracers for biomass combustion and primary bio-particles in atmospheric aerosol, *Atmospheric Environment*, 43, 1367-1371, 10.1016/j.atmosenv.2008.11.020, 2009.
- Johnston, F. H., Hanigan, I. C., Henderson, S. B., Morgan, G. G., Portner, T., Williamson, G. J., and Bowman, D. M. J. S.: Creating an Integrated Historical Record of Extreme Particulate Air Pollution Events in Australian Cities from 1994 to 2007, *Journal of the Air and Waste Management Association*, 61, 390-398, 10.3155/1047-3289.61.4.390, 2011.
- 505 Keywood M D, Hibberd M F, and Emmerson K M: Australia state of the environment 2016: atmosphere, independent report to the Australian Government Minister for the Environment and Energy, Australian Government Department of the Environment and Energy, Canberra, doi:10.4226/94/58b65c70bc372., 2017.
- Keywood M, Selleck P, Galbally I E, Lawson S J, Powell J, Cheng M, Gillett R, Ward J, Harnwell J, Dunne E, Boast K, Reisen F, Molloy S, Griffiths A, Chambers S, Crumeyrolle S, Zhang C, Zeng J, and R, F.: Sydney Particle Study 1 - Aerosol and gas data collectionv3. CSIRO. Data Collection. <https://doi.org/10.4225/08/57903B83D6A5D>, 2016a.
- Keywood M, Selleck, Galbally I E, Lawson S, Powell J, Cheng M, Gillett R, Ward J, Harnwell J, Dunne E, Boast K, Reisen F, Molloy S, Griffiths A, Chambers S, Humphries R, Guerette E, and Cohen D: Sydney Particle Study 2 - Aerosol and gas data collection. v1. CSIRO. Data Collection. <https://doi.org/10.4225/08/5791B5528BD63>, 2016b
- 515 Lawson, S. J., Selleck, P. W., Galbally, I. E., Keywood, M. D., Harvey, M. J., Lerot, C., Helmig, D., and Ristovski, Z.: Seasonal in situ observations of glyoxal and methylglyoxal over the temperate oceans of the Southern Hemisphere, *Atmospheric Chemistry and Physics*, 15, 223-240, 10.5194/acp-15-223-2015, 2015.
- Lim, S. S., Vos, T., Flaxman, A. D., Danaei, G., Shibuya, K., Adair-Rohani, H., Amann, M., Anderson, H. R., Andrews, K. G., Aryee, M., Atkinson, C., Bacchus, L. J., Bahalim, A. N., Balakrishnan, K., Balmes, J., Barker-Collo, S., Baxter,

- 520 A., Bell, M. L., Blore, J. D., Blyth, F., Bonner, C., Borges, G., Bourne, R., Boussinesq, M., Brauer, M., Brooks, P.,
Bruce, N. G., Brunekreef, B., Bryan-Hancock, C., Bucello, C., Buchbinder, R., Bull, F., Burnett, R. T., Byers, T. E.,
Calabria, B., Carapetis, J., Carnahan, E., Chafe, Z., Charlson, F., Chen, H. L., Chen, J. S., Cheng, A. T. A., Child, J.
C., Cohen, A., Colson, K. E., Cowie, B. C., Darby, S., Darling, S., Davis, A., Degenhardt, L., Dentener, F., Des
525 Jarlais, D. C., Devries, K., Dherani, M., Ding, E. L., Dorsey, E. R., Driscoll, T., Edmond, K., Ali, S. E., Engell, R.
E., Erwin, P. J., Fahimi, S., Falder, G., Farzadfar, F., Ferrari, A., Finucane, M. M., Flaxman, S., Fowkes, F. G. R.,
Freedman, G., Freeman, M. K., Gakidou, E., Ghosh, S., Giovannucci, E., Gmel, G., Graham, K., Grainger, R., Grant,
B., Gunnell, D., Gutierrez, H. R., Hall, W., Hoek, H. W., Hogan, A., Hosgood, H. D., Hoy, D., Hu, H., Hubbell, B.
J., Hutchings, S. J., Ibeanusi, S. E., Jacklyn, G. L., Jasrasaria, R., Jonas, J. B., Kan, H. D., Kanis, J. A., Kassebaum,
530 N., Kawakami, N., Khang, Y. H., Khatibzadeh, S., Khoo, J. P., Kok, C., Laden, F., Lalloo, R., Lan, Q., Lathlean, T.,
Leasher, J. L., Leigh, J., Li, Y., Lin, J. K., Lipshultz, S. E., London, S., Lozano, R., Lu, Y., Mak, J., Malekzadeh, R.,
Mallinger, L., Marcenes, W., March, L., Marks, R., Martin, R., McGale, P., McGrath, J., Mehta, S., Mensah, G. A.,
Merriman, T. R., Micha, R., Michaud, C., Mishra, V., Hanafiah, K. M., Mokdad, A. A., Morawska, L., Mozaffarian,
D., Murphy, T., Naghavi, M., Neal, B., Nelson, P. K., Nolla, J. M., Norman, R., Olives, C., Omer, S. B., Orchard, J.,
Osborne, R., Ostro, B., Page, A., Pandey, K. D., Parry, C. D. H., Passmore, E., Patra, J., Pearce, N., Pelizzari, P. M.,
535 Petzold, M., Phillips, M. R., Pope, D., Pope, C. A., Powles, J., Rao, M., Razavi, H., Rehfuess, E. A., Rehm, J. T.,
Ritz, B., Rivara, F. P., Roberts, T., Robinson, C., Rodriguez-Portales, J. A., Romieu, I., Room, R., Rosenfeld, L. C.,
Roy, A., Rushton, L., Salomon, J. A., Sampson, U., Sanchez-Riera, L., Sanman, E., Sapkota, A., Seedat, S., Shi, P.
L., Shield, K., Shivakoti, R., Singh, G. M., Sleet, D. A., Smith, E., Smith, K. R., Stapelberg, N. J. C., Steenland, K.,
Stockl, H., Stovner, L. J., Straif, K., Straney, L., Thurston, G. D., Tran, J. H., Van Dingenen, R., van Donkelaar, A.,
540 Veerman, J. L., Vijayakumar, L., Weintraub, R., Weissman, M. M., White, R. A., Whiteford, H., Wiersma, S. T.,
Wilkinson, J. D., Williams, H. C., Williams, W., Wilson, N., Woolf, A. D., Yip, P., Zielinski, J. M., Lopez, A. D.,
Murray, C. J. L., and Ezzati, M.: A comparative risk assessment of burden of disease and injury attributable to 67 risk
factors and risk factor clusters in 21 regions, 1990-2010: a systematic analysis for the Global Burden of Disease Study
2010, *Lancet*, 380, 2224-2260, 10.1016/s0140-6736(12)61766-8, 2012.
- 545 Millero FJ, Feistel R, Wright D G, and McDougall TJ: The composition of Standard Seawater and the definition of the
Reference-Composition Salinity Scale, *Deep-Sea Research* 55, 50–72., 2008.
- Morille, Y., Haeffelin, M., Drobinski, P., and Pelon, J.: STRAT: An automated algorithm to retrieve the vertical structure of
the atmosphere from single-channel lidar data, *Journal of Atmospheric and Oceanic Technology*, 24, 761-775,
10.1175/jtech2008.1, 2007.
- 550 Norris, G., Vedantham, R., and et, a.: EPA Positive matrix factorization (PMF) 3.0 - Fundamentals and User Guide. US
EAP/600/R-08/108 , Accessed: 15/06/2017, Available: [https://www.epa.gov/air-research/positive-matrix-
factorization-model-environmental-data-analyses](https://www.epa.gov/air-research/positive-matrix-factorization-model-environmental-data-analyses), 2008.
- Pope, C. A., Burnett, R. T., Thun, M. J., Calle, E. E., Krewski, D., Ito, K., and Thurston, G. D.: Lung cancer, cardiopulmonary
mortality, and long-term exposure to fine particulate air pollution, *Jama-Journal of the American Medical
555 Association*, 287, 1132-1141, 10.1001/jama.287.9.1132, 2002.
- Radhi, M., Box, M. A., Box, G. P., Mitchell, R. M., Cohen, D. D., Stelcer, E., and Keywood, M. D.: Size-resolved mass and
chemical properties of dust aerosols from Australia's Lake Eyre Basin, *Atmospheric Environment*, 44, 3519-3528,
10.1016/j.atmosenv.2010.06.016, 2010.
- Schnell, J. L., and Prather, M. J.: Co-occurrence of extremes in surface ozone, particulate matter, and temperature over eastern
560 North America, *Proceedings of the National Academy of Sciences*, 114, 2854-2859, 10.1073/pnas.1614453114, 2017.
- Simoneit, B. R. T., Schauer, J. J., Nolte, C. G., Oros, D. R., Elias, V. O., Fraser, M. P., Rogge, W. F., and Cass, G. R.:
Levoglucosan, a tracer for cellulose in biomass burning and atmospheric particles, *Atmospheric Environment*, 33,
173-182, 10.1016/s1352-2310(98)00145-9, 1999.
- 565 Simoneit, B. R. T.: Biomass burning - A review of organic tracers for smoke from incomplete combustion, *Applied
Geochemistry*, 17, 129-162, 10.1016/s0883-2927(01)00061-0, 2002.
- Weitkamp C: Lidar: Range-Resolved Optical Remote Sensing of the Atmosphere, Springer Series in Optical Sciences,
Springer Science + Business Media, Boca Raton, USA, 2005., 2005.
- Whetton P, Ekstrom M, Gerbing C, Grose M, SBhend J, Webb L, and Risby J (eds): Climate change in Australia: projection
for Australia's natural resource management regions -technical report . CSIRO and BoM, Australia.

570 https://www.climatechangeinaustralia.gov.au/media/ccia/2.1.6/cms_page_media/168/CCIA_2015_NRM_TR_Front_Index.pdf, 2015.

Whittlestone, S., and Zahorowski, W.: Baseline radon detectors for shipboard use: Development and deployment in the First Aerosol Characterization Experiment (ACE 1), *Journal of Geophysical Research-Atmospheres*, 103, 16743-16751, 10.1029/98jd00687, 1998.

575